

M.I. GORBUNOV, M.V. KOVTANETS,  
O.V. SERHIENKO, T.M. KOVTANETS

**DEVELOPMENT AND EVALUATION OF TECHNICAL SOLUTIONS  
TO INCREASE THE QUALITATIVE LEVEL  
OF THE LOCOMOTIVE UNDERCARRIAGE**



Monograph

2021

MINISTRY OF EDUCATION AND SCIENCE OF UKRAINE  
VOLODYMYR DAHL  
EAST UKRAINIAN NATIONAL UNIVERSITY

M.I. GORBUNOV, M.V. KOVTANETS,  
O.V. SERHIENKO, T.M. KOVTANETS

**DEVELOPMENT AND EVALUATION OF  
TECHNICAL SOLUTIONS TO INCREASE  
THE QUALITATIVE LEVEL OF THE  
LOCOMOTIVE UNDERCARRIAGE**

***Monograph***

**Severodonetsk – 2021**

**UDC 625.032.3**  
**G 671**

*This monograph is recommended for printing by the Science  
Council Volodymyr Dahl East Ukrainian National University  
(Protocol № 4 from 26 november 2021 year)*

**Reviewers:**

*Fomin O.V.*, Ph.D., Professor, Professor of Wagons and Carriage  
Management Department, State University of  
Infrastructure and Technology;

*Domin Yu.V.*, Ph.D., Professor, Professor of Railway and Road Transport,  
Lift and Care Systems Department, Volodymyr Dahl East  
Ukrainian National University.

**Gorbunov M.I., Kovtanets M.V., Serhiienko O.V., Kovtanets T.M.**

Development and evaluation of technical solutions to increase the  
qualitative level of the locomotive undercarriage / M.I. Gorbunov,  
M.V. Kovtanets, O.V. Serhiienko, T.M. Kovtanets – Severodonetsk: EUNU, 2021.  
– 94 p.

ISBN 978-617-11-0218-7

The monograph deals with issues of development and evaluation of  
technical solutions that increase the quality level of the locomotive's running gear.  
The evaluation of the effectiveness of the constructive options of nodes and  
devices is carried out with the help of simulation and mathematical modeling  
methods.

**УДК 625.032.3**  
**Г 671**

© Gorbunov M.I., Kovtanets M.V., Serhiienko O.V., Kovtanets T.M., 2021  
**ISBN 978-617-11-0218-7**

## TABLE OF CONTENTS

1. MATHEMATICAL MODELS FOR THE STUDY OF TRACTIVE AND DYNAMIC PERFORMANCE OF VEHICLES .....	6
2. ANALYSIS OF CONTEMPORARY TENDENCIES IN THE ROLLING STOCK DESIGN .....	10
2.1. Increasing the traction performance .....	10
2.2. Improving the dynamics .....	11
2.3. Using the asynchronous drive .....	11
3. METHODS FOR ASSESSING THE TRACTION AND DYNAMIC PROPERTIES OF THE ROLLING STOCK .....	16
4. JUSTIFICATION OF INITIAL BACKGROUND OF THE MATHEMATICAL MODEL OF THE LOCOMOTIVE .....	23
5. FEATURES OF A MATHEMATICAL MODEL OF A SIX-AXLE LOCOMOTIVE'S MOTION .....	26
5.1. Electromagnetic processes modeling in a traction electric drive .....	36
5.2. Disturbances from the track .....	38
5.3. Modeling of longitudinal vibrations in a train .....	40
5.4. Ability of the program to calculate the parameters of the locomotive's motion .....	43
6. ANALYSIS OF THE RESULTS OF CALCULATION OF THE TRACTION AND DYNAMIC QUALITIES OF THE LOCOMOTIVE .....	44
6.1. Testing of the mathematical model of locomotive movement, analysis of the influence of the choice of the adhesion model on the calculation results .....	44
6.2. Influence of the tractive force of a locomotive on the results of calculations of dynamic processes in the «vehicle-track» system .....	54
6.3. Influence of dynamic processes on generation of the tractive force during the locomotive's motion .....	62
6.4. Analysis of the principles of operation of devices that improve the adhesion of the wheels of the locomotive to the rails in traction and braking modes .....	65
6.5. Analysis of the principles of the operation of anti-slipping devices of the locomotive .....	75
CONCLUSIONS .....	82
BIBLIOGRAPHY .....	83
Appendix .....	100

## 1. MATHEMATICAL MODELS FOR THE STUDY OF TRACTIVE AND DYNAMIC PERFORMANCE OF VEHICLES

Theoretical methods for studying the dynamics and tractive properties of the rolling stock, as well as the traction of a locomotive wheel to the rail were extensively studied by A.I. Belyayev, I.V. Biryukov, V.F. Verigo, S.V. Vershynskyy, A.L. Golubenko, L.O. Grachyova, V.N. Danylov, V.D. Danovych, A.S. Yevstratov, V.V. Ivanov, I.P. Isayev, A.A. Kamayev, D.E. Karminskyy, A. Ya. Kohan, A.N. Konyayev, M.L. Korotenko, S.M. Kutsenko, V.A. Lazaryan, A.A. Lvov, V.B. Medel, D.K. Minov, A.P. Pavlenko, T.A. Tibilov, A.N. Savoskin, V.F. Ushkalov, V.D. Khusidov and others, as well as by foreign scholars such as Joly, Kalker, Carter, Krettek, Müller, de Pater and others.

Let us take a look at the current state of mathematical modeling of the movement of rail vehicles so as to study their tractive and dynamic properties.

In the overwhelming majority of cases, the locomotive tractive [23, 31, 51, etc.] and dynamic [12, 23, 31, 51, 76, etc.] performance assessment models are developed separately.

In addition, all of them can be divided by the degree of detail into macro-level models that can be used at the preliminary design stage, and into the more detailed ones that take into account the features and properties of each specific vehicle design.

Various models of locomotives are used while assessing the tractive properties of the vehicles. Factoring in the tractive power is what differs them from the models used in the studies of the dynamics that are considered mostly when the vehicle moves in the coasting mode.

The simplest and most popular are the static models in the vertical plane that are applied in the assessment of the influence of the tractive power on the redistribution of vertical loads along the wheelsets of a locomotive [23, 31, 51]. The tractive effort is assumed to be constant. The criterion for the assessment of the locomotive traction properties in such models is the static coefficient of use of the adhesion weight (1).

The method is simple; it makes it possible to evaluate the influence of the design and characteristics of the connections of the body with the bogies and the bogies with the wheelsets, the layout of the vehicle on the coupling properties of the locomotive, however only approximately, without taking into account the dynamic processes.

When considering the oscillations of a locomotive in the vertical plane, taking into account the constant tractive effort and disturbances from the side of the railway track, more complex mathematical models have been developed [28]. They allow taking into account the influence of the dynamics of the vehicle in the vertical plane on the tractive force implementation process, however disregarding

the electrodynamic processes in the traction drive [56], the mutual influence of the vertical and horizontal oscillations on the adhesive qualities of the locomotive, and vice versa.

In [47], a model of oscillations of a locomotive bogie in the vertical plane is also considered, however taking into account the electrodynamic processes in the traction drive. The focus is made on the influence of the adhesion conditions on the torque transmitted from the traction electric motor armature to the wheelset axle. The influence of the responses in the motor-axle bearings and the suspension of the traction electric motor from the action of the tractive torque and the application of the tractive force on the vertical load of the wheelset on the rails and the significant influence of the vertical oscillations on the magnitude of the tractive force are also noted, which is experimentally confirmed [51]. However, this model also does not take into account the influence of the tractive force on the oscillations in the horizontal plane and the relationship between the vertical and horizontal oscillations.

The spatial oscillations of a wheel-motor unit with rubberized wheels are addressed in [17, 23, 68]. The mathematical model takes into account the tractive torque of the electric motor defined as the ratio of the motor power to the angular speed of rotation of the armature. In this case, the fluctuations in the tractive torque are disregarded; moreover, the behavior of the sprung parts of the body and the bogie is simplified which does not provide a complete picture of the processes occurring in the "vehicle-track" system.

In the mathematical model of vertical oscillations of the wheel-motor unit [31], the oscillations of the tractive torque of the traction electric motor act as a source of disturbances in the presence of the vertical oscillations of the vehicle, and the elasticity of the axle during the torsion is also taken into account. This model is simplified and cannot be used to study the traction properties of the entire locomotive.

The mathematical model of the motion of a single wheelset on a track is addressed in [79] and it is also noted that the tractive torque appears to be the source of external disturbances when a wheelset of a locomotive moves along a straight track section. This model has the same disadvantages as the previous one.

The mathematical models of the "vehicle-traction drive-railway track" are built and analyzed in [56, 55, 57], which makes it possible to evaluate the stability indicators and dynamic qualities of the locomotive in the horizontal plane, taking into account the electrodynamic and mechanical oscillatory processes in the traction drive and control system in the traction and coasting modes. The author of the works [55, 56, 57] concludes that additional disturbing forces appear in the traction mode of the locomotive, causing the horizontal and lateral oscillations of the wheelsets. The above forces are of the same order as the elastic-dissipative forces acting on the wheelsets from the side of the bogies. Due to the effect of the

tractive torque of the traction electric motor on the wheelsets, an additional relationship is established between the horizontal and the vertical oscillations of the sprung and unsprung masses of the vehicles. Furthermore, an important conclusion was made that the critical speed of a rail vehicle in the traction mode can be 12-18% lower than in the coasting mode. However, these works do not assess the adhesion properties of the entire locomotive.

A mathematical model of the horizontal dynamics of a wheelset of an electric locomotive is presented in [49], which includes the equations of motion, the power electric circuit and the electromechanical conversion of energy when the tractive force is applied. The importance of taking into account these processes is noted for the best use of the adhesion in the most severe modes when the locomotive is starting and accelerating. Thus, the task is also to study the influence of the traction torque of the traction electric motor on the horizontal dynamics of the vehicle, but also, as in the previous case, the entire locomotive is not considered.

A mathematical model of spatial oscillations of a locomotive was developed in [14, 15], taking into account the tractive force. It considers the interrelation of all processes occurring during the oscillations of the vehicle in different planes, but does not take into account the electrodynamic processes in the traction drive and the longitudinal oscillations of the train set.

Mathematical models for studying the dynamics of railway vehicles are divided into linearized and non-linearized. The former are used to assess the stability of motion; for them, a solution can be obtained in an analytical form; the latter are the closer to the real structures and take into account nonlinearities and evaluate the dynamics of motion. They are solved mainly by numerical methods. In addition, both of these and other locomotion models can be flat (in vertical or horizontal planes) or spatial.

However, most models of locomotive dynamics, especially horizontal dynamics [51, 76], are based on the assumption that the locomotive moves at a constant speed. This assumption excludes the consideration of processes occurring in the longitudinal direction, i.e. acceleration, deceleration, longitudinal oscillations and, consequently, the tractive force and the tractive torque. At the same time, according to the results of the experimental [14, 15, 42, 84, 88] and theoretical works [14, 15, 55, 56, 57], one may conclude about the influence of processes in the traction drive and in the contact between the wheel and the rail under the impact of tractive forces on the dynamics of the locomotive.

Therefore, to study the traction qualities of locomotives, mathematical models of spatial oscillations have been developed, however disregarding the electrodynamic processes in the traction drive. The mathematical models that take into account these processes are built, as a rule, only for the oscillations of the vehicle in the vertical plane.

In most cases, the dynamic qualities of locomotives are studied using the mathematical models of the movement of vehicles that are built without regard to the tractive force.

Based on this, it is necessary to consider the following:

- 1) A mathematical model of a locomotive to assess its traction and dynamic qualities must take into account the spatial oscillations of the vehicle;
- 2) The model must be built taking into account the traction torque and electrodynamic processes in the drive;
- 3) The simulation models built on the basis of experimental data will be more reliable.



## **2. ANALYSIS OF CONTEMPORARY TENDENCIES IN THE ROLLING STOCK DESIGN**

### **2.1. Increasing the traction performance**

The literature data analysis provides insight into various methods that are known to improve the adhesion of the wheels to the rails when the locomotive moves in the traction and the braking modes. Let us highlight the most common ones:

- Redistribution of vertical loads over wheelsets during the traction and braking in order to balance them out [22, 29, 51];
- Redistribution of tractive (braking) forces across the wheelsets of a locomotive, depending on the vertical loads or the slipping [22, 29, 54];
- Use of traction electric motors with more stringent characteristics, including asynchronous ones [60, 65];
- Use of devices for feeding the abrasive materials into the contact between the wheel and the rail (sandboxes);
- Use of slipping control systems in the wheel-rail contact [46, 85].

In the early 1990s, the EMD electric traction division of General Motors (USA) and Siemens (Germany) began production of new SD60MAC and SD70MAC freight diesel locomotives with an AC drive with a capacity of 4,000 hp [46]. The first one weighs 177 tons, the second is 188 tons. In the process of their creation, a number of points of interest moments arose, associated precisely with the development process. The system that controls the slip between the wheels and the rail is particularly interesting [46]. The speed of the locomotive is measured by a radar. The optimum wheel slip measuring device automatically finds the appropriate operating mode based on the traction or the brake force set by the driver, and by the feedback signals. Wheel slip regulators act on the control system of each of the traction inverters. When the condition of the rails deteriorates, the device decreases the preset value of the slipping speed. Depending on the tractive force, speed and condition of the rails, the slipping speed can vary within the range of 6% to 24%.

Whenever the radar fails, the information about the speed is obtained by the pseudo-runner axle method that compares the angular speeds of rotation of the locomotive wheelsets. This method is less accurate than the previous one, so it is only used as a last resort.

Therefore, the optimum traction and braking qualities of the modern rolling stock should be ensured in all possible ways from the design of the drive and to dedicated anti-slide and anti-slip devices.

The advantages of the traction qualities of locomotives with an asynchronous drive were proven in practice [46] in 1992 during the tests on the ring of the Pueblo Test Center (Colorado, USA). It was found that three SD60MAC locomotives

could replace the five SD40-2 DC locomotives commonly used to haul heavy coal trains on the Burlington Norton track. By using the modern diesel locomotives, the railway operator was able to reduce its locomotive fleet and cut the operating costs.

In practice, the adhesion coefficients ranging from 0.35 to 0.45 have been achieved. These high coefficients were achieved through the use of an asynchronous drive and bogies with radially directed wheels in the curved sections of the railway track, which made it possible, on the one hand, to reduce the dynamic forces while moving along the curved tracks, and, on the other hand, to reduce the resistance to motion.

This is due to a significant improvement in the adhesion properties of a fundamentally new locomotive (formerly, the adhesion limitation had a stronger negative impact on the properties of the locomotive than the power limitation).

The new locomotives will help increase the train mass by 15-25%. This is indicative of the reserves for using the power of the traction rolling stock that may be tapped through the effective use of the vehicle traction capacity.

Demonstration trips were conducted along nine major rail roads in the United States and Canada for six months of 1993. It was one of the most intense demonstration of the traction rolling stock.

## **2.2. Improving the Dynamics**

The use of bogies equipped with wheels that are radially guided in the curved tracks [46] allows, on the one hand, reducing the dynamic forces during the motion in the curved tracks, and, on the other hand, reducing the resistance to motion. In addition, this practically helped achieve the adhesion coefficients ranging between 0.35 and 0.45 [46].

## **2.3. Using the asynchronous drive**

Modern locomotives and electric trains in Europe are currently running on the AC transmission. The new traction rolling stock considerably changes the conditions of transportation and the train driving practices. These changes are so important that they are compared with the transition from steam to diesel propulsion. The asynchronous drive has a number of significant advantages, which has been repeatedly proven in practice.

This was influenced by the fact that due to the improved design and control system, the power transmission, primarily an asynchronous drive, now possesses a number of indisputable advantages as follows:

- The power transmission provides for the better use of power at the start from standstill, when the tractive force drops slightly, until the hyperbolic part of the characteristic ( $P = \text{const}$ ) is reached, where the electric transmission secures a hyperbolic traction property, which is a

prerequisite for the better utilization of power. This considerably improves the acceleration and the speed properties of the train set;

- The average operational efficiency of a diesel locomotive equipped with power transmission (with similar motors) is higher than the efficiency of a diesel locomotive equipped with other types of transmissions, both due to the higher efficiency of the transmission itself and a good match of the properties of the power transmission and diesel engine;
- The possibility of energy recovery during the braking with an electric brake system which allows using up to 12% of the energy [35];
- The minimized depreciation in comparison with other types of transmissions due to the very small number of parts subject to wear;
- Favorable conditions for maintenance secured by the opportunity for rational arrangement of all machinery and hardware;
- Reliable operation of the diesel engine secured by the elimination of critical revolutions and reloads;
- Good throttle response and the ability to reverse promptly and to control the speed smoothly.

The operation of an asynchronous traction motor (ATM) both in the electrically propelled stock (EPS) and in the diesel trains was for a long time hindered by the level of development of semiconductor technology (there were no reliable and effective AC frequency converters) and only after the appearance of power semiconductor control devices - thyristors, the extensive application of the ATM in electric traction has become an issue. This gave the following advantages over commutator motors:

- Power and ATE torque increased 1.5-2 times, while reducing the mass (by 30%-40%) and overall dimensions (no collector and winding needed). In terms of individual power, the ATE is 2-2.5 times higher than commutator motors;
- Improved EPS propulsion properties through the better use of the wheel-to-rail adhesion, thanks to the rigid traction during the slipping. According to the calculations 5, the use of ATE increases the adhesive weight utilization factor from 0.90 to 0.98, which is confirmed by the experimental data where the adhesion coefficient increases by 20%-40%;
- The EPS operation costs reduced by a simpler design of the ATE in comparison with commutator motors and the increased reliability of the body electrical equipment.

The absence of a commutator-brush assembly not only increases the reliability of the ATM, but also makes the maintenance thereof in the course of operation easier, because one no longer needs to inspect the collector-brush assembly on a daily basis. In addition, an ATM with a short-circuited rotor has only one stator winding with insulation, therefore it does not require periodic

inspections by qualified mechanics, and its maintenance is reduced only to packing grease into the bearings. The use of non-contact power converters increases the reliability of the body electrical equipment.

For example, according to VVS, the total cost of operation of the E-1200 electric locomotives equipped with asynchronous traction motors are half of those of EA-1000 electric locomotives with commutator motors, due to the following factors:

- Significant reduction in the consumption of non-ferrous metal, insulation and electrical steel. For example, manufacturing the latest ATM requires 2-2.5 times less copper than manufacturing commutator motors;
- The use of ATM provides for complete automation of the train driving mode.

Fig. 1 represents the traction characteristics of a diesel train with a hydraulic transmission DR1M (with two hydraulic torque converters) and the expected traction characteristic of a diesel train with an ATM power transmission designed at the LTZ, reduced to the power of a diesel train DR1M (1,000 hp) at the same power for auxiliary needs, as well as the curves of the efficiency of the electric and hydraulic transmission of these diesel trains.

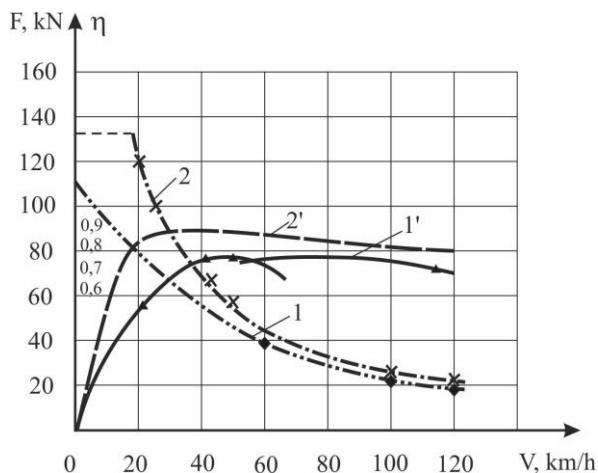


Fig. 1. Traction characteristics and transmission efficiency of the diesel train DR1-DR1-1; 1') and the diesel train with an asynchronous drive (2, 2') projected at PO

«Luhanskteplovoz» 1; 1' - characteristics of the diesel train DR1M; 2, 2' - characteristics of a diesel train with an asynchronous drive

According to Fig. 1, the torque on the ATM shaft, along with the tangential tractive force and the speed of the diesel train, depend not on the characteristics of

the diesel engine but rather on the power and the electrical parameters of the generator and the ATM; therefore, their value can be changed by adjusting the level and the phase voltage frequency  $U$ . If one takes into account that the efficiency of the diesel operation at a reduced capacity is determined by the nature of the dependence of the generator resistance moment  $M_g = f(n)$ , which, in turn, depends on the magnetic flux caused by the loading of traction motors, then the automatic regulation of the electrical parameters of the ATM and the generator (depending on the angular speed) may ensure the operation of any diesel engine with the greatest efficiency in the entire range of the operating speeds.

Until recently, such control conditions could not be implemented, but with the emerging industrial static semiconductor converters one can successfully solve this problem. In this case, the traction characteristics slightly differ from the ideal hyperbolic constant power curve (see Fig. 1); these variations are due to the change in the efficiency of the traction generator and the electric motor, i.e. the change in the efficiency of the electric transmission in the range of speeds.

Therefore, the electrical drive of asynchronous frequency-regulated short-circuited rotor tractive motor ensures the required traction performance within the entire adjustment range with minimal losses in traction motors while ensuring economical, smooth operation of the diesel engine within the entire gear range, without switching gears. For example, in terms of the overall size and weight of diesel locomotives and diesel trains with hydraulic transmission, which often requires room for a refrigerator and drive shafts, they differ little from diesel locomotives and diesel-powered trains with power transmission from ATE, the weight of which can be significantly reduced due to the fact that there is no need for the collector and windings of the additional poles and the compensating coil, and by reducing the weight of the motor frame, which is not a magnetic circuit, the strength of which can be ensured by the choice of materials and the use of stiffeners.

In addition, the use of the ATM group power supply wherein the frequency and voltage for the motors of each bogie are the same, allows the use of the natural stiffness of the ATM traction feature at a constant stator current frequency, which provides better anti-slipping properties when the wheel-rail adhesion is disrupted, the motor speed and the associated wheel slipping speed on which the coefficient of adhesion depends change insignificantly, thereby excluding any chance of a random slipping and makes it possible to realize the maximum tractive forces in terms of adhesion. The possibility of redistributing the electrical load of the ATM depending on the wheel diameter and the statistical load from the axle to the rail both at the time of the take off and during the driving increases the coefficient of use of the adhesion mass of a diesel train, which, in combination with the rigid characteristics of the ATD, provides for better traction properties than even a mono-motor drive, because the difference in the diameters of the wheelset rims

with a mono-motor drive increases the resistance to the motion, and the total tractive force on the wheelsets in this case is smaller than in the ATM drive.

Reducing the cost of the electrical drive with the ATM through considerably reduced consumption of non-ferrous metal, insulation and electrical steel, and implementation of high capacities and torques, compactness, reliability and ease of operation would minimize the advantages of the hydraulic transmission in terms of similar indicators. Based on the foregoing, when choosing a gear for a diesel train, the use of an asynchronous drive appears to be feasible.

According to experimental measurements of the coefficient of adhesion on electric and diesel locomotives operated by the German railways [90], the maximum coefficient of adhesion of rolling stock is 0.30-0.33, but some locomotives with traction motors having more rigid characteristics and a perfect control system for traction electric motors are persistently demonstrating the bigger values of the coefficient of adhesion. For example, the E1200 electric locomotive with asynchronous traction motors has a friction coefficient of 0.419. Similar data on electric locomotives E1200, VL80a and VL86f with asynchronous traction motors are provided in [78].

### 3. METHODS FOR ASSESSING THE TRACTION AND DYNAMIC PROPERTIES OF THE ROLLING STOCK

The traction properties of locomotives are assessed by experimental and theoretical methods.

Experimental evaluation is an expensive and time-consuming process and is possible only if there is a full-scale sample or a physical model of the locomotive. Following the years of research and generalization of experimental data, one would usually get the empirical expressions for determining the design and regulatory coefficient of adhesion for various types of locomotives [24, 62].

Theoretical methods, in turn, can be divided into quantitative and qualitative.

Qualitative assessment of the adhesion properties is based on the analysis and generalization of the experimental data and theoretical studies. For example, it was found that a locomotive with a group drive of wheelsets has better adhesion than an individual drive [24]. However, there may be opposite conclusions as well [34, 42]. The same can be said about the advantage of the balanced bogie suspension over the individual suspension, etc.

Quantitatively, the adhesion properties of a rail vehicle are usually assessed by the following indicators:

1. The static coefficient of the use of adhesion weight per wheelset [24, 31, 51, 65]

$$\eta_u = \frac{P - \Delta P}{P},$$

where  $P$  - vertical load from the wheelset on the rails;

$\Delta P$  - change in the vertical load from the wheelset on the rails.

The dynamic nature of the change in vertical loads, the torque of the motors and the change in the frictional properties of the wheel-rail contact are not taken into account in this case.

2. Adhesion weight utilization rate [63]

$$\eta = \frac{\psi}{\psi_o}, \quad (1)$$

where  $\psi$  - coefficient of adhesion of the locomotive,

$\psi_o$  - coefficient of adhesion of the axle that went into slipping.

Let us analyze this criterion

$$\psi_o = \frac{F_o}{P_o}, \psi = \frac{F}{P},$$

where  $F_o$ ,  $F$  - respectively, the adhesion force of the limiting axle of the locomotive and the average adhesion force per axle;

$P_o$ ,  $P$  - the vertical load from the limiting axle on the rails and the average vertical load of the locomotive from the axle on the rails.

The limiting wheelset is the wheelset in the vehicle that is most prone to slipping (sliding).

If we proceed on the assumption that the de facto adhesion force on all wheelsets of the locomotive is the same, i.e.  $F_o = F$ , this indicator really evaluates the use of the adhesion weight. However, due to the unequal adhesion conditions on each axle (vertical loads, frictional conditions, dynamic forces), the adhesion forces on each axle vary [23]. Therefore, this criterion reflects the ratio for conditions of adhesion on the limiting wheelset to the conditions for the entire locomotive, or, in other words, the tendency of the locomotive to slipping (sliding). Let us call it the adhesion utilization factor. It allows one to judge the tractive force generated by the locomotive under various driving conditions, however, it does not take into account the dynamic nature of the change in vertical loads and the adhesion forces.

3. The tractive coefficient, defined as the ratio of the actual tractive force to the adhesion weight of the locomotive [40, 45, 65]. The tractive force generated by the locomotive depends on the speed, frictional conditions, irregularity and the track profile and is a variable value. In some cases [45], the tractive force of the design mode is assumed, however it would be impossible to assess the adhesive performance at the take off, during the braking and at the speeds other than the long-term.

4. The generated coefficient of adhesion  $\psi_{STS}$ , which is characterized by the statistical law of distribution [65] or the ratio of the calculated value to the potentially possible (physical) value [21] or the adhesion area [6]. In all these cases, the change in the adhesion coefficient in relation to the design features of the vehicle is not taken into account, and the concept of a potentially possible (physical) adhesion coefficient, which depends on many factors and is a random value, is not defined.

5. The adhesion utilization coefficient as an indicator characterizing the degree of reduction of the limiting traction capabilities of a wheelset, determined by the maximum possible (potential) coefficient of adhesion [23]. The



disadvantage of this criterion also comes from the uncertain concept that is referred to as the maximum possible adhesion coefficient.

6. Adhesion utilization coefficient during the braking, which equals to the ratio of the acting braking forces to the forces of adhesion of the wheels to the rails during the braking period, [2]. This criterion was proposed for the assessment of braking qualities of the newly created vehicles.

7. The adhesion utilization coefficient in traction, which can be obtained through a similar approach for the traction mode, defined as the ratio of the tractive force of a locomotive on the track section to the tractive force of the wheels on the rails. The disadvantage of this criterion is that the concept of adhesion forces between the wheels and the rails is not clearly defined [2], since the magnitude of the adhesion force in contact between the wheels and the rails is determined by the magnitude of the traction or braking force on the wheel rim.

8. The maximum tractive force on the coupler, which a locomotive can develop for a long time without slipping [47]. All the above criteria for evaluating the coupling properties of a locomotive make it possible to only indirectly judge the tractive force that a locomotive can generate, since the magnitude of this force is influenced by many factors. Therefore, an integral criterion is used, the choice of which is justified by the target function of the locomotive - to perform the maximum possible work on a given section of the track, which is fully characterized by the tractive force averaged over the section

$$F_o = \frac{1}{T_o} \int_0^{T_o} \left( \sum_{i=1}^n P_i(t) \psi_i(V_{CK}(t)) \right) dt, \quad (2)$$

where  $T_o$  - the time of movement along the section of the track;

$n$  - the number of wheels of the driving axles;

$P_i$  - the vertical load from the wheel on the rail;

$\psi_i$  - the coefficient of adhesion of a wheel to a rail.

This approach seems to be the most reasonable, since the tractive force that a locomotive can generate is estimated directly. This approach, however, still has certain drawbacks. Under good frictional conditions, two different locomotives can generate the same tractive force, and when conditions deteriorate, these tractive forces will be different due to their varying tendencies to slipping.

In this work, as in the case considered hereinabove, the average tractive force which the locomotive is capable of developing over the section of motion for a long time without slipping represents a criterion for the tractive performance of the locomotive

$$F_o = \frac{1}{T_o} \int_0^{T_o} \left( \sum_{i=1}^n F_{xi} \right) dt, \quad (3)$$

with the only difference that it is defined as the sum of the longitudinal adhesion forces of the wheelsets of the locomotive to the rails averaged over the section  $F_{xi}$  (this approach is based on the fact that the useful tractive force is generated only through the longitudinal components of the adhesion forces).  $F_{xi}$  determined in the process of solving the contact problem of rolling a locomotive wheel on a rail, taking into account the experimental dependencies [18, 19, 41].

The exact display in the mathematical model of the conditions of contact interaction between the wheels and the rails allows evaluating the adhesion qualities of the compared structures directly by the maximum tangential tractive force, which can be achieved through the contact. This value equals the maximum adhesion force  $F_{ad \max}$  of the wheel and is numerically determined by integrating the shearing stresses over the contact area [42].

The value of  $F_{ad \max}$  depends on the frictional state of the contacting surfaces, the mechanical properties of the materials of the wheel and the rail, the power loads, the kinematic and dynamic features of the motion. In this work, the problem of simultaneous consideration of all these factors is solved through finding the solutions to equations that describe the motion of a locomotive, therefore, a criterion for assessing the traction capabilities of a locomotive is used by the maximum traction it develops.

Two locomotives of different design can achieve the same tractive force value under the similar driving conditions (primarily frictional) and completely different under other conditions, which is associated with the design features of the vehicle, and above all, with the different tendency of the rail vehicle to slipping (slipping). When the locomotive moves in a traction mode, each driving wheelset has its own coefficient of adhesion. This is caused by the difference in vertical loads, frictional conditions, traction moments, design and operational features of the vehicles. If the coefficient of adhesion of one of the wheelsets is overestimated in relation to the coefficients of adhesion of the other wheelsets and the entire locomotive, then it will go into slipping (sliding) faster than the other axes with an increase in the tractive moment or with a deterioration in the frictional contact conditions. This wheelset is the limiting one. The ratio of the locomotive adhesion coefficient to the limiting axle adhesion coefficient makes it possible to assess the tendency of the latter to go slipping (sliding). Therefore, the third criterion for assessing the traction qualities was adopted - the adhesion utilization coefficient (when moving in traction and in braking modes) (1), however taking into account the dynamic processes during the motion of the vehicle:

$$\psi_O = \frac{\frac{1}{T_O} \int_0^{T_0} (\sum_{i=1}^n F_{xi}) dt}{\frac{1}{T_O} \int_0^{T_0} (\sum_{i=1}^n P_i) dt}, \psi = \frac{\frac{1}{T_O} \int_0^{T_0} (\sum_{i=1}^n F_{li}) dt}{\frac{1}{T_O} \int_0^{T_0} (\sum_{i=1}^n P_{li}) dt} \quad (4)$$

Here  $F_{lx}$  and  $P_l$  - the adhesion forces and the vertical load of the limiting wheelset.

The lower the ratio (1), the higher the friction coefficient of the limiting axle compared to the friction coefficient of the locomotive and the other axles, the more the locomotive will be prone to slipping. Ideally, this ratio should equal to one. With this kind of ratio, all wheelsets will have the same tendency to slipping (slipping) and the locomotive will be able to achieve its maximum tractive force under the worse frictional conditions than a locomotive with a limiting wheelset. The range of the maximum power utilization by the locomotive will increase. The ways to achieve this will be described below.

But none of these criteria can fully characterize the traction qualities of a locomotive. The state when  $F_{xi} = F_{ad \max}$ , i.e. the maximum on the adhesion characteristic determines the unstable mode of tractive force generation, because with the slightest increase in the tractive moment between the wheel and the rail there occurs a complete relative slippage of the surfaces, i.e. slipping, which leads to an increase in inertia forces that are dangerous for a traction electric motor (TEM) and to the increased wear of the contacting surfaces of the wheels and rails, the development of frictional self-oscillations, at which the maximum dynamic moments in drives are several times higher than the maximum adhesion values [21, 56]. Therefore, it is necessary to evaluate the tractive force that is consistently generated by the locomotive.

In works [14, 22, 68], it was experimentally and theoretically shown that with an increase in the dynamic forces of interaction between a locomotive wheel and a rail, the adhesion conditions get worse. When generating the same tractive force

$F_T$ , the value of the slip gets higher with an increase in dynamic forces  $\mathcal{E}$  (Fig. 2). The conditions for generation of the tractive force and the traction qualities of the locomotive get worse with every increase in the value of the slip. Therefore, a criterion is needed that would characterize precisely the contact of the wheel with the rail.

For this, [14, 15] suggest one to consider directly the processes in the contact of the wheel with the rail, specifically, the relationship between the zones of adhesion and slipping, when assessing the traction qualities of a locomotive. This criterion, from the point of view of the author, can characterize the process of wheel-to-rail adhesion more accurately. However, the implementation of this

method is difficult on ordinary computers due to the large volume of computational operations. In addition, at present, it is practically impossible to experimentally confirm the results of theoretical calculations.

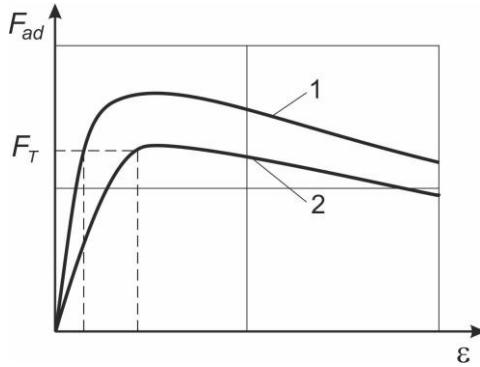


Fig. 2. Influence of the dynamic forces in the "wheel-rail" system on the amount of slipping during the generation of the tractive effort; 1 - characteristic of adhesion in the absence of dynamic forces, 2 - in the presence of dynamic forces (according to [138])

In a simplified form, this can be done using the ratio  $\varepsilon/\varepsilon_{kp}$ , which characterizes the margin of sustainable generation of the tractive force of the locomotive ( $\varepsilon$  - the value of the relative slip of the wheel of the locomotive on the rail;  $\varepsilon_{kr}$  - critical slip corresponding to the maximum value of the adhesion). At  $\varepsilon/\varepsilon_{kr} = 1$  the reserve of sustainable tractive force will be chosen and any further increase in traction will send it into the slipping mode.

The dynamic qualities of the vehicle are most often assessed by the following indicators:

1. Horizontal  $k_{dg}$  and vertical  $k_{DV}$  dynamics [9, 10, 12, 51, 31]

$$k_{DV} = F_{DV} / F_{ST}, \quad k_{dg} = F_{dg} / F_{st}, \quad (5)$$

where  $F_{DV}$ ,  $F_{dg}$  - dynamic vertical and horizontal force components that occur in individual spring suspension kits;

$F_{st}$  - static load in the same spring suspension kits;

$k_{dg}$ ,  $k_{DV}$  - the coefficients of horizontal and vertical dynamics which can also be determined through deformations, characterizing the impact on the vehicle, although they do not take into account the frequency spectrum of the vibrations affecting the person and the vehicle.

2. Maximum accelerations and travel of the body and other elements of the vehicle [10, 12, 31, 51, 66]. This criterion has the same advantages and disadvantages as the previous one.
3. Smoothness indicators determined by the values of vibration and acceleration frequencies [10, 12, 31, 51]. In this case, the frequency spectrum of vibrations, the impact on the person and the vehicle are taken into account, but the magnitude of the effective forces is not estimated.
4. Dynamic stability. This criterion is specific for horizontal shear vibrations and wobble vibrations [9, 26, 50, 31, 76].
5. Based on the comprehensive criterion for evaluating the lateral vibrations of a locomotive, formulated and mathematically substantiated by V.A. Lazaryan in [14], the essence of which is as follows: asymptotic stability of unperturbed motion is necessary, and the minimum level of forces caused by external disturbances is a sufficient condition for good dynamic qualities of a rail vehicle when moving within the sub-critical range of speeds. This criterion also applies only to wobble oscillations.
6. Directly by the magnitude of horizontal and vertical forces acting on units and structural elements of a rail vehicle [30, 31, 39, 67, 76]. This approach does not take into account the frequency spectrum of vibrations, but allows one to assess the dynamic impact on the entire vehicle and on its individual elements.
7. Values of the guiding efforts. This criterion is similar to the previous one and characterizes the interaction between the wheel and the rail in the transverse direction, and assesses the safety of the motion.
8. Values of the edge stress. This approach also characterizes only the interaction between the wheel and the rail.

In this work, the dynamic qualities of a locomotive are assessed by the values of forces and accelerations, the coefficients of horizontal and vertical dynamics, all of which are most widely used. In addition, there is the richest experimental material on them.

#### **4. JUSTIFICATION OF INITIAL BACKGROUND OF THE MATHEMATICAL MODEL OF THE LOCOMOTIVE**

The parameters of the 2TE-116 diesel locomotive were taken as benchmark data for the calculations (see Appendix). The calculations were carried out for one section.

The coefficient  $S$  that influences the amplitudes of the horizontal irregularities of the track is set at 0.8, for vertical irregularities  $S = 1.4$ .

As mentioned hereinabove, design of a locomotive involves the search for solution to a complex problem - simultaneous attainment of the optimum traction and dynamic qualities.

In the practice of modeling dynamic processes during the motion of railway vehicles, especially in the domestic practice, in most cases, modeling of oscillations in the vertical and horizontal planes proceeds separately. However, this approach does not quite correctly reflect the physical processes.

The vertical and horizontal vibrations of the vehicle are kinematically related, since the rolling surfaces of the rim and the rail have a non-cylindrical shape and any travel thereof in the horizontal plane will cause vertical vibrations. In turn, oscillatory processes in the vertical plane and in the longitudinal direction largely determine the values of the forces of interaction between the wheel and the rail, which directly affect the behavior of the vehicle in the horizontal plane.

One can expect an increase in the mutual influence of processes in the vertical and horizontal planes with an increase in the speeds of motion of the rail vehicles. Therefore, to improve the accuracy of calculations, a spatial model of locomotive motion shall be used [14, 22, 66].

In most works devoted to the problems of the locomotive's motion stability, it is assumed that the locomotive moves in the coasting mode [31, 43, 51, 57], and the traction torque and electromechanical processes in the traction drive do not affect the dynamics of the locomotive. At the same time, the mathematical models of the movement of a locomotive and a carriage practically do not differ from each other. However, it was shown above that the torque from the traction motors acting on the wheelset has a significant effect on the stability of its motion and horizontal dynamics. This is confirmed by the field test results [14, 43, 84, 88].

For example, in 1982, during the traction tests carried out by the VNITI on the Railway Research Institute (VNIIZhT) loop, experiments were carried out on TEM2 locomotive No. 7024 to compare the trajectories of the locomotive's wheelset in the traction and the stopping modes. We measured the lateral travel of the wheelset relative to the railway track on a straight section 500 m long. According to the research, when the locomotive moves in a traction mode, the wheelset moves with large transverse amplitudes, and the mathematical expectations of the wobble wavelength are less (by about 18-20%) than when stopping [14, 43].

Other studies [27, 56, 55, 57, 84, 88] have shown that the tractive force and the power drive performance have a direct impact on the dynamics of the locomotive, and the traction qualities are directly related to the dynamic properties [51, 63]. This means that a more reliable description of the processes occurring when the locomotive moves in various modes would require the introduction of a traction source - a traction drive - into the relevant mathematical model.

When modeling the motion of a locomotive, it is often assumed that it moves at a constant speed [28, 51, 57, 76, etc.] and the longitudinal vibrations do not affect the nature of its behavior. In this case, it is assumed that  $V = \omega R = \text{const}$ . Then the angular velocity of rotation of the wheels and, consequently,  $\varepsilon_x$ , shall be determined only by the speed of translational motion and the kinematics of the wheelset, i.e. the difference in wheel diameters and the difference in the distance traveled by the right and the left wheels in a wheelset when moving in a curve.

At the same time, for the locomotive, the slip  $\varepsilon_x$  is also the result of the action of the tractive force. Therefore, the abovementioned assumption that excludes the action of the tractive force on  $\varepsilon_x$  and  $\omega$ , can be permissible for studying the stability of motion of non-traction rail vehicles, but not justified when studying the motion of a locomotive operating for a considerable time under conditions of traction and braking.

While modeling the motion of a locomotive, the matter of forces in the contact of a wheel with a rail [16, 43, 72, 73, 87] is of great importance as well.

Thus, in [16], the analysis of the influence of the methods for modeling the forces of pseudo-sliding was carried out on the example of a single wheelset motion model. Models were used in accordance with the theories of Carter [81], Kalker [38, 83] and Frederich [82]. The studies have shown differences in the behavior of a wheelset with different representations of tractive forces: The results of theoretical studies that are closest to the experimental data were obtained using the models that take into account the forces in the wheel-rail contact according to the Kalker theory. In [50, 72, 73], the results of calculations of the motion of the freight, passenger and motor carriages of an electric train were analyzed using various adhesion models [50, 53, 86]. They also showed significant discrepancies.

For example, the difference in adhesion forces reaches 50%, and for the body movements - 11% [73]. Taking into account the considerable dependence of the results of solving the problem of interaction between the vehicles and the track by the method that takes into account the forces of pseudo-sliding, it was concluded that in the study of oscillations of the rolling stock, one should generally use the more accurate nonlinear hypotheses of creep, taking into account the slipping and the dynamic load on the rail [50, 72]. However, these studies covered only the vehicles and disregarded the effect of the traction moment.

In [87], the motion of a single wheelset with conical rims on a railway track at a speed of up to 60 m/s and various values of the torque ranging from 0 to 2 kNm was considered. The Frederich adhesion model [82] was used. The

calculation results for the kinematics of the wheelset motion in this case better correspond to the real situation than for the linearized mathematical model.

Longitudinal vibrations of locomotives and carriages greatly influence the generation of the tractive force. In transient modes of movement, the longitudinal forces in the train (at the coupler) can significantly (several times) exceed the maximum developed tractive force of the locomotive [8, 7, 10, 51]. Hence the importance of taking these processes into account when studying the traction and the dynamic properties of the rolling stock.

The torsional stiffness of the axle has a significant effect on the forces of frictional interaction in the contact between the wheels and the rails [63, 77].

Therefore, when modeling the motion of a locomotive, it is important to take into account the traction moment, a method for mathematical modeling of the frictional interaction between the wheel and the rail, and the longitudinal dynamics of a train. These factors significantly affect the behavior of the locomotive when it moves on a railway track.



## 5. FEATURES OF A MATHEMATICAL MODEL OF A SIX-AXLE LOCOMOTIVE MOTION

Taking into account the results obtained in Chapter 3 and Chapter 4, and the analysis of impact of the most significant factors on the nature of the motion of the locomotive, the following prerequisites were laid in the basis for the construction of a mathematical model of a six-axle locomotive motion:

1. Spatial vibrations are considered.
2. The motion of two sections of a six-axle locomotive on a track section of an arbitrary outline in the plan is studied.
3. All bodies of the system (locomotive body, bogie frames, traction motors (TED), wheelsets and rims) are assumed to be absolutely rigid.
4. Nonlinearities in the axle boxes during the lateral runs of the wheelsets, in pivot assemblies when carrying bogies, in body supports on a bogie with the rocking vehicle, were taken into account.
5. The action of friction elements in the axle box spring suspension is considered.
6. The force of resistance to the motion of the locomotive and train is taken into account.
7. The calculations are carried out when the locomotive is moving in the coasting, traction and braking mode.
8. The adhesion force is determined separately for each wheel, depending on the vehicle speed, the sliding speed of contacting bodies, the vertical load, frictional state, the wheel and the rail profiles, and their relative position. Various models of frictional interaction are used to represent the adhesion force between the wheel and the rail (4, 15, 38).
9. The longitudinal speed of the locomotive is determined in the process of integrating the differential equations of motion and no restrictions are imposed on its value.
10. The track is considered in the form of discrete inertial beams of infinite length, lying on an elastic-dissipative [75] or elastic-viscous [9, 12] base, under the action of vertical and lateral horizontal forces applied at the points of contact between the wheels and rails. Dissipativity is taken into account by dry friction forces [75], viscosity is taken into account by the drag coefficient  $\varepsilon_x$  [9, 12]. The reduced track mass is assumed to be constant [9, 10, 12]. The path stiffness values are taken according to [9, 10, 75].
11. The rim and the rail have arbitrary profiles.
12. The friction of the wheel flange on the rail is taken into account when choosing a clearance in the railway track.
13. Electrodynamic processes during the motor operation are taken into account.

14. Longitudinal vibrations of the train are taken into account during the motion.

15. The torsional stiffness of the wheelset axle is taken into account.

Fig. 3 shows a general view of the considered model (one section). symbols of the movement of all bodies of the system are summarized in Table. 1.

T a b l e 1

**Symbols for the movement of all bodies of the system**

	Movements					
	linear, along the axes			angular, relative to the axes		
	$OX$	$OY$	$OZ$	$OX$	$OY$	$OZ$
Body	$x_b$	$y_b$	$z_b$	$\theta_b$	$\varphi_b$	$\psi_b$
Bogie frame		$y_{TK}$	$z_{TK}$	$\theta_{TK}$	$\varphi_{TK}$	$\psi_{TK}$
Wheelsets	$x_{wi}$	$y_{wi}$	$z_{wi}$	$\theta_{wi}$	$\varphi_{wi}$	$\psi_{wii}$
Motor						$\psi_{mi}$
Armature						$\psi_{ai}$
Rails at the contact points		$y_{pij}$	$z_{pij}$			

Here  $k = 1, 2$  - bogie number;

$i = 1.2 \dots 6$  - the number of the wheelset in the locomotive; indices (  $j = 1$  ) right and left, (  $j = 2$  ) sides in the direction of travel, in addition,  $m = 1, 2, 3, 4$  are used to indicate the number of the body support on the bogie.

The following restrictions are imposed on the movement of the bodies in the system:

1. While in motion, the wheel does not come off the rail surface. Then the vertical travel of the rail lines are as follows

$$Z_{pij} = Z_{rimij} + \delta R_{ij} ,$$

where  $Z_{rimij}$  - the vertical travel of the rims,

$\delta R_{ij}$  - the changes in the rolling radius of the wheel. For the linear profile of wheels

$$\delta R_{ij} = (-1)^{j+1} \lambda y_{rimij} ,$$

$$\delta R_{ij} = f_1(y_{rimij}).$$

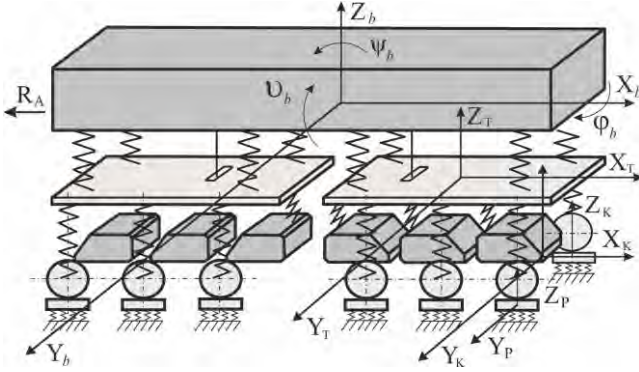


Fig. 3. Design model of spatial vibrations of a 6-axle locomotive

Specific kind of function  $f_1$  for various combinations of wheel and rail profiles are set forth in [41]

2. The bracings between the body and the bogies in the longitudinal direction is absolutely rigid, i.e.  $x_b = x_{T1} = x_{T2}$ .
3. With axial support, the traction motor is rigidly connected to the axle of the wheelset, except for the rotation about the axis  $OY$ .
4. The traction motor armature in the housing can only rotate about the axis  $OY$ , the traction drive is rigid.
5. The travel of the tracks occurs in two directions - along the axes  $OY$  and  $OZ$ .
6. The wheelset is assumed to be an absolutely rigid body; only the torsional stiffness of the axle is taken into account.

There are 21 bodies in the system (body, two bogies, six traction motors, six traction motor armatures, six wheelsets), and each of them has six degrees of freedom. The rails under each wheel have two degrees of freedom (a discrete model of the track is considered). Taking into account the available bracings, the system has  $21 \cdot 6 + 6 + 12 \cdot 2 - 12 \cdot 1 - 2 \cdot 1 - 6 \cdot 5 - 6 \cdot 6 = 76$  degrees of freedom. Its behavior is described by differential equations of the second order. In addition, to determine the traction moment, the currents in the traction motor circuits are to be found, which means 6 more generalized coordinates. The second section of locomotives has the same number of bracings. When modeling the train composition for each

car, only longitudinal vibrations are considered, and since the number of cars  $N$  can be arbitrary, then  $N$  generalized coordinates are added.

The symbols for the linear, inertial, stiffness and damping parameters of the locomotive are summarized in Table. 2.

T a b l e 2

**Symbols for locomotive parameters**

No.	Name	Symbol
1	2	3
1.	Half the distance between the wheel rolling circles	$S$
2.	Half the distance between the axle boxes in the transverse direction	$l_{by}$
3.	Distance between the axle boxes in the bogie in the longitudinal direction	$l_{bx}$
4.	Half the distance between the supports in the transverse direction	$l_{sy}$
5.	Half the distance between the supports in the bogies in the longitudinal direction	$l_{sx}$
6.	Distance between the axle and the traction motor suspension	$l_{tr}$
7.	Distance between the axis and the center of gravity of the traction motor	$l_{tr}$
8.	Distance between the center of the bogie and the center pin	$l_{cp}$
9.	Distance between the center of the body and the center pin	$l_{cpk}$
10.	Axial gear ratio	$\mu$
12.	Wheelset mass	$m_k$
13.	Traction motor mass	$m_{tm}$
14.	Bogie mass	$m_T$
15.	Body mass	$m_b$
16.	Moments of inertia relative to the axis $OX$ :	
	wheelset	$l_{wx}$
	motor	$l_{tmx}$
	bogie	$l_{Tx}$
	body	$l_{bx}$

Table 2 continued

1	2	3
17.	Moments of inertia relative to the axis $OY$ :	
	wheelset	$l_{wy}$
	motor	$l_{tmy}$
	armature	$l_{ay}$
	bogie	$l_{Ty}$
	body	$l_{by}$
18.	Moments of inertia relative to the axis $OZ$ :	
	wheelset	$l_{wz}$
	motor	$l_{tmz}$
	bogie	$l_{Tz}$
	body	$l_{bz}$
19.	Reduced rail mass	$m_p$
20.	Stiffness of axle suspension elements (per one axle):	
	longitudinal	$S_{Bx}$
	transverse before taking up the elastic play	$S_{By1}$
	transverse after taking up the elastic play	$S_{By2}$
	vertical	$S_{Bz}$
21.	Stiffness of the elements of the second stage of spring suspension (per one support):	
	longitudinal	$S_{supx}$
	transverse	$S_{supy}$
	vertical	$S_{supz}$
22.	Traction motor suspension stiffness:	
	transverse	$S_{msy}$
	vertical	$S_{msz}$
23.	Center pin stiffness:	
	with a clearance of up to 20 mm	$S_{cp1}$
	with a clearance of 20 mm to 40 mm	$S_{cp2}$
24.	Rail line stiffness:	

Table 2 continued

1	2	3
	vertical	$S_{pz}$
	transverse	$S_{py}$

The stationary coordinate system begins at the center of gravity of the body at the moment of equilibrium and rest (Fig. 3), so that the axis  $OX$  parallel to the rails with a positive direction that matches the travel, axis  $OZ$  in the same longitudinal plane with a positive upward direction, axis  $OY$  - perpendicular to the previous one with a positive direction rightwards, when viewed in the direction of the travel. The positive direction of the angles and moments is clockwise.

Normally, the position of the body and the associated travel coordinate system with respect to the stationary system can be determined by three linear coordinates of the point  $O_1 - x, y, z$  and three Euler angles  $\varphi, \psi, \theta$  of rotation of the moving coordinate system relative to the stationary one.

Therefore, as a moving coordinate system, we take the system  $O_1x_1y_1z_1$ . System  $O_1x_1y_1z_1$  performs both the progressive and the rotational movement in the angle  $\varphi, \psi$  and  $\theta$ , and determines the relative travel of the wheelset.

The coordinate systems are connected by using the transition formulas known in mechanics, the coefficients of which are represented by the cosines of the angles between the corresponding axes. To switch from the natural axes in system  $O_1x_1y_1z_1$  to the coordinate system  $Oxyz$ , we use the following formulas:

$$\begin{aligned} x &= a_{11}x_1 + a_{12}y_1 + a_{13}z_1 \\ y &= a_{21}x_1 + a_{22}y_1 + a_{23}z_1 \\ z &= a_{31}x_1 + a_{32}y_1 + a_{33}z_1 \end{aligned}$$

Cosine values  $a_{ij}$  are summarized in Table 3

Table 3

The value of the cosines  $a_{ij}$ 

	$x_2$	$y_2$	$z_2$
$x_1$	$\cos \psi$	$-\varphi$	$\sin \psi$
$y_1$	$\varphi$	1	$-\theta$
$z_1$	$-\sin \varphi$	$\theta$	$\cos \psi$

Lateral deformations of the body supports on the bogie

$$\Delta_{yij} = y_b + (-1)^{k+1} \varphi_b l_{opxb} - (y_{tk} + (-1)^m \varphi_{tk} l_{opxt}) .$$

7. The force of dry friction of the wheel flange against the rail head is taken into account when the wheelset takes up the clearance in the track.
8. A traction moment is applied to the wheelset.
9. No restrictions are imposed on the change in the traveling speed.
10. A motion resistance force is applied to the wheelset.

The angular movement of the bogies about the axis  $OZ$  is as follows:

$$\Delta_{\varphi k} = \varphi_b - \varphi_{tk}$$

The vertical deformations of the body supports on the bogie are as follows:

$$\Delta_{zizj} = z_b + (-1)^j \theta_b l_{opy} + (-1)^k \psi_b l_{opxk3} - (z_{tk} + (-1)^j \theta_{tk} l_{opy} + (-1)^m \psi_{tk} l_{opxt}) .$$

The movement of the center pin relative to the bogie is as follows:

$$\Delta_{cp} = y_b + (-1)^{k+1} \varphi_b l_{cpk} - (y_{tk} + (-1)^k \varphi_{tk} l_{cp}) .$$

The movements of the axle boxes of the wheelsets relative to the bogie frames in the longitudinal direction are as follows:

$$\Delta_{Bxij} = x_{tk} + (-1)^j \varphi_{tk} l_{By} - (x_{wi} + (-1)^j \varphi_{wi} l_{By}) .$$

The movements of the axle boxes of the wheelsets relative to the bogie frames in the transverse direction are as follows:

$$\Delta_{Byyi} = y_{tk} + (-1)^{k1} \varphi_{tk} l_{Bxx} - y_{wi} ,$$

where  $k1=1$  for the 1st and the 4th wheelsets and  $k1=2$  for the 3rd and the 6th wheelsets.

The movements of the axle boxes of the wheelsets relative to the bogie frames in the vertical direction are as follows:

$$\Delta_{Bzij} = z_{tk} + (-1)^j \theta_{tk} l_{By} + (-1)^{k1} \psi_{tk} l_{Bxx} - (z_{Bij} + (-1)^j \theta_{Bij} l_{By}) ,$$

where  $k1=1$  for the 1st and the 4th wheelsets and  $k1=2$  for the 3rd and the 6th wheelsets.

The elastic deformations of the traction motor suspension in the transverse direction is as follows:

$$\Delta_{msysy} = y_{rk} + (-1)^{k1} \varphi_{rk} (l_{Bxx} + (-1)^{k2} l_{lm}) - (y_{wi} + (-1)^k \varphi_{wi} l_{lm}),$$

where  $k1=1$  for the 1st, the 4th and the 5th wheelsets and  $k1=2$  for the 2nd, the 3rd and the 6th wheelsets,  $k2=1$  for the 1st and the 6th wheelsets and  $k2=2$  for the 2nd, the 3rd, the 4th and the 5th wheelsets.

The responses of most elastic links in the system are linearly dependent on the travels. Exceptions:

1. The transverse responses of the axle box spring suspension (Fig. 4) is as follows:

$$R_{Byyi} = \dot{\Delta}_{Byyi} \beta_{By1} + \Delta_{Byyi} \alpha_{By1} + ((\Delta_{Byyi} - \Delta_{Bi} \text{sign}(\Delta_{Byyi})) S_{By2} + \dot{\Delta}_{Byyi} \beta_{By1}) \text{sign}(b1_i),$$

where  $S_{By1}$ ,  $S_{By2}$  - the lateral stiffness of the elastic elements of the axle box spring suspension before taking up the elastic clearance in the axle box and after taking up the elastic play;

$\beta_{By1}$  - the viscous friction coefficient of the elastic bracing of the axle box spring suspension in the transverse direction before and after taking up the elastic play;

$\text{sign}(b1_i)$  equals 1 when  $\Delta_{Byi}$  exceeds the elastic play and is equal to 0 as long as the elastic play is not taken up.

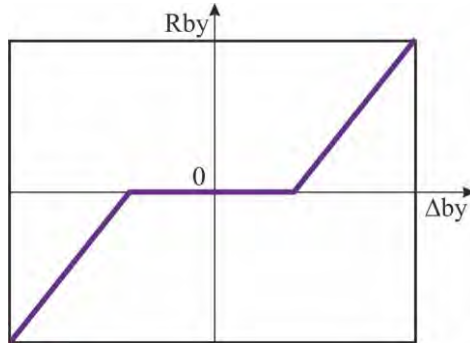


Fig. 4. Transverse responses of the axle box spring suspension



2. The resistance force of the friction vibration damper in the axle box stage of the spring suspension is as follows:

$$F_{cij} = F_{tp} \text{sign}(\dot{\Delta}_{Bzij}),$$

where  $F_{tp}$  is the frictional force of the absorber.

3. The moment of resistance of the body supports on the bogie when turning about the axis (Fig. 5) is as follows:

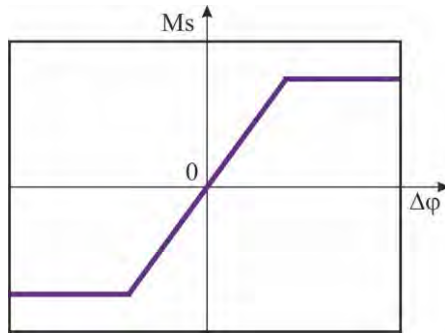


Fig. 5. The moment of resistance to the rotation of the body supports on the bogie

$$\begin{aligned} R_{\text{sup}\varphi k} &= \dot{\Delta}_{\text{sup}\varphi k} \beta_{\text{sup}\varphi} + \Delta_{\text{sup}\varphi k} S_{\text{sup}\varphi} \quad \text{at } \Delta_{\text{sup}\varphi k} \leq \varphi_{\text{res}}; \\ R_{\text{sup}\varphi k} &= M_{\text{res}} \quad \text{at } \Delta_{\text{sup}\varphi k} > \varphi_{\text{res}}, \end{aligned}$$

where  $S_{\text{sup}\varphi}$  - the stiffness of the elastic elements of the body supports on the bogie when the bogie is turning about the axis  $OZ$  ;

$\beta_{\text{sup}\varphi}$  - the viscous friction coefficient of the elastic elements of the body supports on the bogie when turning about the axis  $OZ$  ;

$M_{\text{res}}$  - the restoring moment arising in the roller devices of the supports;

$\varphi_{\text{res}}$  - the angle of rotation of the bogie relative to the body before turning on the roller devices.

4. The transverse responses of the center pin mechanism (Fig. 6) is as follows.

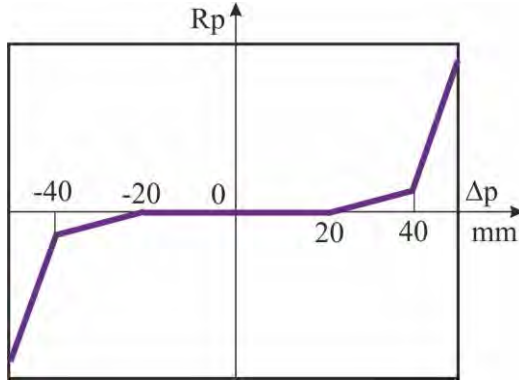


Fig. 6. Transverse responses of the pivot device

$$R_{cpy} = \dot{\Delta}_{cpy} \beta_{cpy1} + \Delta_{cpy} \kappa_{cpy1} + (\dot{\Delta}_{cpy} \beta_{cpy2} + (\Delta_{cpy} - \Delta_{cp1} \text{sign}cp) S_{cpy2}) \text{sign}cp1_w + (\Delta_{cpy} - \Delta_{cp2} \text{sign}cp) S_{cpy3} \text{sign}cp2_w,$$

where  $S_{cpy1}$ ,  $S_{cpy2}$ ,  $S_{cpy3}$  - the lateral stiffness of the elastic elements of the center pin mechanism when the center pin moves relative to the bogie up to 20 mm, of 20 mm to 40 mm, and over 40 mm, respectively;

$\beta_{cpy1}$ ,  $\beta_{cpy2}$  - the viscous friction coefficients of the elastic elements of the center pin mechanism, respectively, when the center pin moves relative to the bogie up to 20 mm and from 20 to 40 mm, respectively.

5. The lateral force acting from the side of the rail on the wheel is as follows:

$$R_{pyij} = -0.5((\dot{y}_{pyi1} \beta_{py} + y_{pyi1} S_{py})(1 + \text{sign}(y_i)) + (\dot{y}_{pyi2} \beta_{pyi2} S_{py})(1 - \text{sign}(y_i))) \text{sign}(d_i),$$

where  $S_{py}$  - the transverse stiffness of the rail line;

$\beta_{py}$  - the viscous friction coefficient of the sub-rail base in the transverse direction;

$\text{sign}(d_i)$  equals 1 when taking up the clearance on the railway track, and equals 0 until the clearance is taken up. When taking up the clearance, the rail and

the wheel move simultaneously, i.e.  $y_{pij} = y_{ij} - \Delta$  at  $y_{ij} - y_{pij} \geq \Delta$ , where  $\Delta$  is the clearance on the railway track.

These responses are used as summarized forces in the system of differential equations of the locomotive motion.

To compose it, the Lagrange equations of the second kind were used. The system of differential equations is presented as follows

$$[M]\{\ddot{q}\} + [B]\{\dot{q}\} + [K]\{q\} = \{Q(t)\},$$

where  $[M], [B], [K]$  - the matrices of the inertial, dissipative and elastic coefficients, respectively;

$\{\ddot{q}\}, \{\dot{q}\}, \{q\}$  - the vectors of accelerations, velocities and travels of bodies in generalized coordinates;

$\{Q(t)\}$  - the vector of summarized forces. The coefficients of the matrices and summarized forces are set forth in Appendix 2.

The solution of the equations is in the time domain in the form of a state vector  $\{x\}$  is as follows:

$$\{x\} = \begin{Bmatrix} \dot{q} \\ q \end{Bmatrix}$$

### 5.1. Electromagnetic processes modeling in a traction electric drive

When determining the traction moment, electrodynamic processes in the traction electric drive are taken into account. For this, the equations of the dynamics of a series-wound traction motor (Fig. 7) are as follows:

$$\frac{di_{ai}}{dt} = \frac{1}{L_1} (U_o - i_{ai} R_1 - e),$$

$$M_{eli} = c_m \Phi i_{ai},$$

$$e = c_e \Phi \dot{\psi}_{ai},$$

where  $i_{ai}$  - armature current;

$L_1$  - inductance of the motor circuit;

$U_o$  - source voltage;

$R_1$  - resistance of the motor circuit;

$e$  - rotational electromotive force;

$\Phi$  - magnetic flux;

$M_{eli}$  - torque on the motor shaft;

$C_M$  and  $C_e$  - constant of the motor.

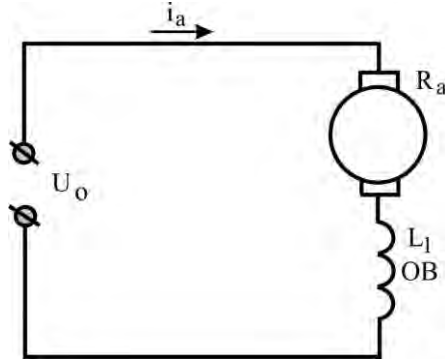


Fig. 7. Wiring diagram of a series-wound DC traction motor

The characteristics of the traction generator of the 2TE10V, 2TE10M diesel locomotives or the selective characteristics of the 2TE116 traction generator [11, 77] are approximated by the function

$$U_o = \begin{cases} 700 & \text{if } i = 2530 \\ 1720000 / i & \text{if } 2530 \leq i \leq 6200 \\ i & \text{not more } 6200. \end{cases}$$

A value equal to  $e / \dot{\psi}_{ai}$ , [11], with a high degree of accuracy for traction electric motors ED-108A, ED-118A (diesel locomotives 2TE10V, 2TE10M, 2TE116) is approximated as follows

$$f(i_a) = 8,5(1 - \exp(-i_a / 400)).$$

Then

$$\begin{aligned} \frac{di_{ai}}{dt} &= \frac{1}{L_1} (U_o - i_{ai} R_1 - f(i_{ai}) \mu \dot{\psi}_{ai}), \\ M_{eli} &= f(i_{ai}) \mu i_{ai}, \end{aligned}$$

where  $\mu$  - the gear ratio of the traction reducer.

## 5.2. Disturbances from the railway track

When a locomotive moves on a railway track, free and forced vibrations occur. To determine the dynamic performance of the vehicle, the mode of steady-state forced oscillations is considered [51].

One of the main sources of disturbances in the simulation of the "vehicle-track" system is considered to be the disturbances coming from the track.

A real railway track is a spatial line with random components and a wide range of irregularities. The changes in the stiffness and geometric characteristics along the length of the track are random and depend on many factors such as the variability of inertial and dissipative properties, track design, system and quality of its maintenance and repair, season, climatic conditions, wear rate, rail sagging, etc.

In most works on the dynamics of rail vehicles [9, 14, 51, etc.], the variability of the properties of the track along its length is set as some kind of an equivalent geometric irregularity  $\eta(x)$ , which takes into account all the reasons that cause disturbing movements.

In many works, horizontal and vertical disturbances are set as harmonic functions, which are periodic irregularities of varying lengths and amplitudes [9, 14, 51]. Such irregularities are considered predominant both in the vertical and in the horizontal plane. To this end, [2] takes into account in  $\eta(x)$  the change in stiffness along the length of the rails in the area of the joints, the change in stiffness in the middle part of the link and the corrugated rail wear: group of irregularities with wavelength of  $L = 0.03-0.08$  m, irregularities with  $L = 0.08-0.3$  m, and irregularities with  $L = 0.6-2.3$  m. Their combination determines the total disturbance originating in the track.

It is impossible to give an exhaustive analytical description of the track; therefore, one has to resort to the statistical description thereof. Present-day works mostly focus on specification of disturbances in the form of random functions [25, 50, 51, 75, 76], since this kind of description is more consistent with reality.

The statistical description of disturbances should contain data on the wavelength of irregularities and on their amplitude. [12] makes a conclusion that a periodically modulated random process is an adequate regularity of typical changes in the geometric parameters of a track. This process comprises two components: a stationary random process that describes random irregularities of a rail and a periodic process that describes regularly spaced rail joints, with a mean amplitude of deviations other than nil, and the said amplitude of deviations changes according to a random law, while the position of the joint remains unchanged.

[48, 75] proceed in a manner that is based on the method of canonical decompositions, which forms a random process with a deterministic periodogram, i.e. the resulting disturbance is the sum of a finite number of the constant length

harmonics with a random amplitude. The disadvantage of this method lies in the limitation of the spectrum of disturbance frequencies.

In [36], the disturbance is modeled on the basis of the Fourier inversion by the sliding summation method. The sliding summation method is approximate due to the methodical error.

[50] is concerned with the analysis of disturbances influencing the vehicle, and the study of problems of the random disturbance modeling in the vertical and horizontal planes. Algorithms are described, and a comparison of methods for random process modeling with arbitrary spectral densities is provided: sliding summation method, canonical decomposition method in various modifications, Rice-Pearson method.

To simulate real disturbances affecting the rail vehicles, an algorithm is applied that involves the use of shaping filters, making it possible to generate a disturbance within a given time interval.

In [26, 25, 50, 61, 76], preference is given to the method of the "white noise" passing through the linear filter. This method is in good agreement with the experimental data [26], satisfying almost the entire range of the railway track disturbances, and is adopted for modeling disturbances from the track side in this work.

In the developed mathematical model of locomotive motion, the disturbing effect from the track is set by the functions of longitudinal travel  $\eta_z(x)$  (in vertical plane) and  $\eta_y(x)$  (in horizontal plane). Functions  $\eta_z(x)$  and  $\eta_y(x)$  are determined independently from each other. Calculations can be performed both for deterministic assignment of disturbances and for a random one.

The deterministic disturbances are specified in the form of sinusoidal functions of the type as follows:

$$\eta(x) = \sum_{i=1}^N A_i \sin(\pi x / L_i)$$

where  $A_i$  is the amplitude of the irregularity;

$L_i$ , - the wavelength of the irregularity.

Random disturbances are specified by the method of the "white noise" passing through the linear filter, which is often used and described in [26, 25, 50, 76]. According to [1, 7], plausible processes  $\eta(x)$  are generated by simulations using the following spectral density expression:

$$S(\omega) = \frac{K}{\gamma^2 + \omega^2},$$

where  $K$  - the coefficient associated with the amplitude of the irregularity;  
 $\gamma$  - current frequency,  $\gamma < \omega$ .

To generate the processes  $\eta(x)$  with spectral density of  $S(\omega)$ , one would normally use the shaping filters of the first order that correspond to the differential equations

$$\dot{y}(t) = -Ay(t) + W(t), \quad \dot{z}(t) = -Az(t) + W(t),$$

where  $A = 2\pi V\omega$ ;  $y(t)$  and  $z(t)$  - random variables;

$W(t)$  - white noise.

The "white noise" signal was modeled using a generator of random numbers uniformly distributed over the interval  $[-1, 1]$ .

The irregularities under the right and the left wheels in the wheelset are not interrelated. For subsequent wheelsets, transport lag is taken into account.  
 $\tau = l_{bi} / V$ .

### 5.3. Modeling longitudinal vibrations in a train set

When studying longitudinal vibrations of a train, two modes of motion are considered:

- The steady mode that takes place with a constant or slow change of forces external to the train. In this case, the forces in the shock-traction devices are determined mainly by these external forces (tangential forces of traction or braking, resistance to motion) and the inertia forces of the cars;
- The unsteady mode that occurs with a sharp transition of the system from one state to another - when starting off, sharp change in the tractive force or braking, moving along a broken profile.

In the steady mode, the train can be considered as a flexible inextensible rod or as a chain of articulated rigid bodies (cars), the relative travels of which can be neglected [10]. Then the equation of the motion of the train will look as follows:

$$\sum_{i=1}^n m_i \ddot{x} = F_k - \sum_{i=1}^n W_i,$$

where  $m_i$  - the mass of the carriage;

$F_k$  - tangential tractive force of the locomotive;

$W$  - the force of resistance to movement, including the locomotive;

$n$  - the number of cars comprising the train.

At transient modes of movement, significant longitudinal vibrations develop in the train. In this case, the longitudinal forces on the automatic coupler can significantly (several times) exceed the tractive force developed by the locomotive [7, 10, 12, 51].

Transient processes are influenced by clearances in the coupling devices and the train is considered as a system of rigid bodies linked into a chain by nonlinear elements (carriages connected by automatic couplings, Fig. 8)

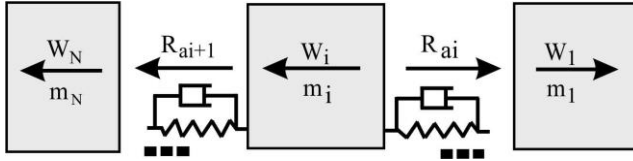


Fig. 8. Pattern of longitudinal forces acting on a carriage as part of the train

$$m_i \ddot{x} = R_{ai} - R_{ai+1} + W_i + F_k, \quad i = 1, n,$$

where  $R_{ai}$  - the forces acting in the elements connecting the bodies in a chain (automatic couplings);  $F_k = F_k$  for the locomotive and  $F_k = 0$  for the carriages.

$$W_i = m_{ei} (a_o + b_o |x_i| + c_o |x_i|^2) \text{sign}(\dot{x}) + j m_{ei};$$

where  $a_o, b_o, c_o$  - - the coefficients of specific resistance to the movement of the carriage [10, 62];

$j$  - the slope of the track.

For freight trains equipped with automatic couplings complete with spring-friction shock absorbing devices with clearances in the coupling, the power characteristics of the carriage-to-carriage coupling are shown in Fig. 9.



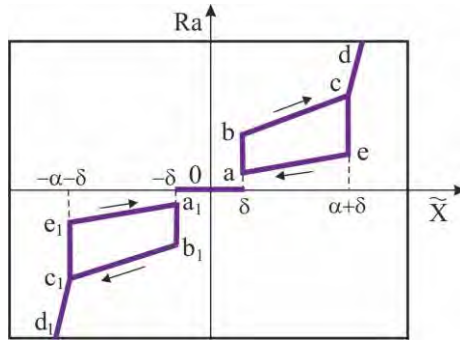


Fig. 9. Power characteristics of the automatic coupler

Modeling the operation of such a system is addressed in [7, 5, 6, 51]. The power characteristics of the carriage-to-carriage coupling is as follows:

$$R_a = \begin{cases} 0, & \text{npu } |x| < \delta \\ \frac{a_1 + b_1 |\dot{x}|}{c_1 + d_1 |\dot{x}|} (N_1 + k_1 (|x| - \delta)) \text{sign}(x), & \text{npu } \delta \leq |x| < a + \delta \text{ u } \dot{x} > 0 \\ \frac{a_2 + b_2 |\dot{x}|}{c_2 + d_2 |\dot{x}|} (N_2 + k_2 (|x| - \delta)) \text{sign}(x), & \text{npu } \delta \leq |x| < a + \delta \text{ u } \dot{x} < 0 \\ (N_3 + k_3 (|x| - a - \delta)) \text{sign}(x), & \text{npu } x > a + \delta, \end{cases}$$

where  $N_1, N_2, N_3$  - the longitudinal forces corresponding to the points  $a, b, c$  ;

$k_1, k_2, k_3$  - the coefficients of the power characteristics of the segments  $bc, ac$  and  $cd$  [10].

For random disturbances, with the exception of the extreme values, one should estimate the mathematical expectations and standard deviations. The mathematical expectation  $\bar{x}$  and the standard deviation  $\sigma_x$  of the process under consideration shall be determined as follows

$$\bar{x} = \frac{1}{N} \sum_{i=1}^N x_i;$$

$$\sigma_x = \sqrt{D_x}, \quad D_x = \frac{1}{N} \sum_{i=1}^N x_i^2 - \bar{x}^2;$$

where  $N$  - the sample size;

$x$  - the value of the random process in  $i$  – th moment in time.

The developed program makes provisions for changing the model for determining the adhesion forces in contact between the wheels and the rails, the profile of the rolling surface of the wheels, the stiffness of the axle box and the central suspension, axial clearances and other design features of the locomotive, the ability to control traction moments, change the traction characteristics of the motors, vertical loads from the wheelsets on the rails, as well as the number of cars comprising the train, the frictional state of the contacting surfaces of the wheels and rails in order to study their influence on the traction and the dynamic qualities of the locomotive.

#### **5.4. Program's features in calculating the parameters of the locomotive's motion**

On the basis of the described mathematical model, a program has been developed for studying the three-dimensional vibrations of a locomotive moving in various modes along a section of the track of an arbitrary profile in the plan. The developed program makes it possible to study the three-dimensional vibrations of locomotives in the modes of traction, coasting and electrodynamic braking.

Research is focusing on a solution to the system of differential equations -  $2 \cdot 158 + 2N$  degree depending on the number of carriages in the train. The solution is carried out by the Runge-Kutta numerical method of the fourth order.

The integration of differential equations helps calculate all linear and angular travels of the body, bogie frames, wheelsets and traction motors, currents in the motor circuits, adhesion forces in contact between the wheels and the rails, vertical and transverse horizontal travels of the rails, longitudinal travels of the cars, as well as the corresponding velocities and accelerations of the bodies of the system. The data obtained in this way are used to determine the values characterizing the dynamic and tractive qualities of the locomotive. These are: the frame and the lateral forces, the vertical forces in contact, the axle box spring suspension and the body supports on the bogies, vertical and lateral horizontal accelerations of the body and bogie frames, wheel slip on rails, angular velocities and accelerations of wheelsets, axle twisting angles, adhesion forces, traction moments, current strength in traction motor circuits.

In order to assess the dynamic and adhesion characteristics of the locomotive in the steady modes of motion, the maximum and the minimum values of all output parameters are determined.

## 6. ANALYSIS OF THE RESULTS OF CALCULATION OF THE TRACTION AND DYNAMIC QUALITIES OF THE LOCOMOTIVE

### 6.1. Testing the mathematical model of the locomotive's motion, analyzing the influence of the choice of the adhesion model on the calculation data

To check the adequacy of the mathematical model of the locomotive's motion and to compare the influence of different adhesion models on the results of the traction and dynamic calculations, a number of problems were considered:

- Coasting of the locomotive;
- Movement of the locomotive in traction mode on the site;
- Hitting an oil slick when the locomotive is moving in traction mode at maximum power;
- Starting of the locomotive from standstill with a train of carriages.

The calculation data of the dynamic processes obtained in solving the first problem were tested by comparison with the results of the running trials of diesel locomotives 2TE-116 No. 517 and No. 1012, carried out by the department of dynamic and strength tests of HC Luhanskteplovoy [67] and the All-Russian Scientific Research Diesel Locomotive Institute (Kolomna) [37]. The test results are summarized in Tables 4 and 5.

T a b l e 4

**Comparison between the calculation and experimental data in terms of the values of the coefficients of horizontal and vertical dynamics**

Experiment [67]				Calculation			
$v$ , m/s	16.7	22.2	27.8	Model	16.7	22.2	27.8
$k_{dg}$	0.07	0.1	0.14	[18]	0.085	0.111	0.143
				[83]	0.133	0.128	0.174
				[81]	0.141	0.130	0.157
$k_{dv}$	0.15	0.16	0.18		0.155	0.167	0.183

Table 5

**Comparison of the maximum frame forces ( $R_{by}$ , kN) obtained during the running trials of 2TE-116 locomotives and the estimates of mathematical expectations of their maximum values**

Wheelset number								
	1		4		5		6	
v, m/s	experiment	calculation	experiment	calculation	experiment	calculation	experiment	calculation
11.1	1) 7.5	4) 7.31	1) 11.0	4) 3.82	1) 8.0	4) 8.92	1) 8.0	4) 9.88
	2) -	5) 12.10	2) -	5) 10.60	2) -	5) 17.26	2) -	5) 18.77
	3) -	6) 15.75	3) -	6) 17.56	3) -	6) 17.95	3) -	6) 19.03
16.7	1) 10.0	4) 11.85	1) 14.0	4) 7.47	1) 11.0	4) 11.06	1) 14.0	4) 14.68
	2) 11.0	5) 17.88	2) 11.0	5) 16.53	2) 9.0	5) 18.85	2) 8.0	5) 23.94
	3) 15.0	6) 23.40	3) 12.0	6) 17.55	3) 13.0	6) 20.84	3) 12.0	6) 25.45
22.2	1) 13.0	4) 12.75	1) 18.0	4) 15.49	1) 14.0	4) 17.57	1) 22.0	4) 20.00
	2) 15.0	5) 13.34	2) 17.0	5) 17.93	2) 13.0	5) 14.72	2) 18.0	5) 22.91
	3) 14.0	6) 17.5	3) 17.0	6) 21.50	3) 14.0	6) 18.61	3) 22.0	6) 23.45
25.0	1) 14.9	4) 18.26	1) 21.0	4) 17.93	1) 16.0	4) 20.56	1) 27.0	4) 22.39
	2) -	5) 22.83	2) -	5) 25.29	2) -	5) 23.36	2) -	5) 27.94
	3) -	6) 27.05	3) -	6) 27.78	3) -	6) 27.18	3) -	6) 29.71
27.8	1) 22.0	4) 20.41	1) 24.0	4) 24.83	1) 17.0	4) 21.75	1) 32.0	4) 25.71
	2) 16.0	5) 22.48	2) 13.0	5) 25.60	2) 14.0	5) 21.96	2) 14.0	5) 27.94
	3) 18.0	6) 28.13	3) 17.0	6) 28.08	3) 19.0	6) 27.62	3) 30.0	6) 29.71
33.3	1) -	4) 25.24	1) -	4) 22.00	1) -	4) 17.86	1) -	4) 24.13
	2) 13.0	5) 22.51	2) 9.0	5) 19.25	2) 13.0	5) 13.32	2) 12.0	5) 24.15
	3) 17.0	6) 19.53	3) 12.0	6) 20.71	3) 15.0	6) 13.23	3) 14.0	6) 22.25

1) - [37], 2) - [67], running forward, 3) - [67], running backward (numbering of wheelsets in the direction of the locomotive's motion), 4) - [18], 5) - [83], 6) - [81]

The analysis of the results in Tables 4, 5, in Figs. 10, 11 demonstrates their satisfactory convergence with the experimental data on the values of frame forces, coefficients of vertical and horizontal dynamics, vertical and horizontal accelerations of the bogies and the body. Moreover, the closest to the experimental data are the estimates obtained using the adhesion model [18].

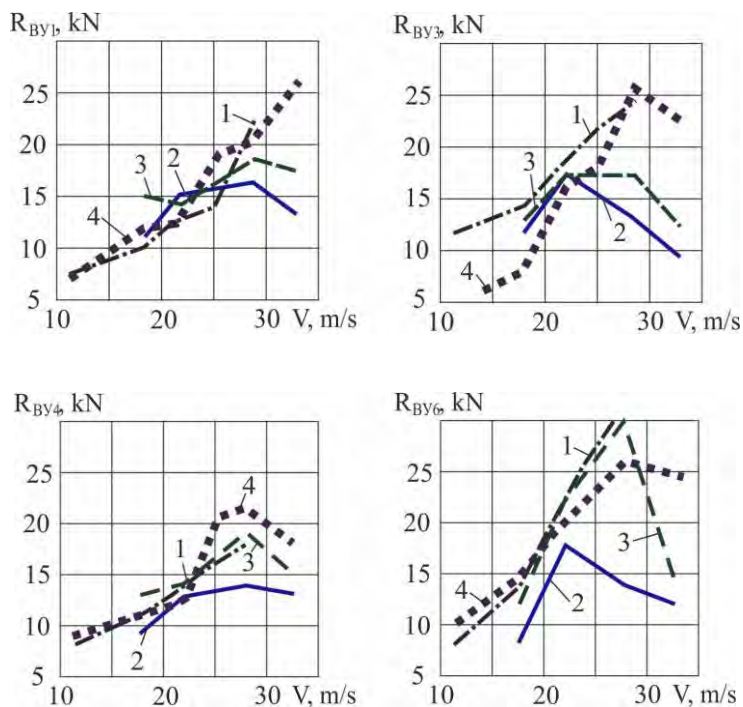


Fig. 10. The maximum frame forces obtained during the running tests of the 2TE116 locomotive (1 - [37], 2, 3 - [67]) and the results of the estimates of mathematical expectations of their maximum values - 4 (model [18]) when coasting

It should be noted that the calculation data of the dynamic processes in the vertical plane when simulating the coasting do not depend on the choice of the adhesion model. The same result was obtained in [72, 73]. This is due to the fact that  $F_{sc}$  acts in a horizontal plane and does not directly affect the vertical vibrations, whereas the vertical forces mostly depend on the locomotive's parameters and the track in a vertical plane.

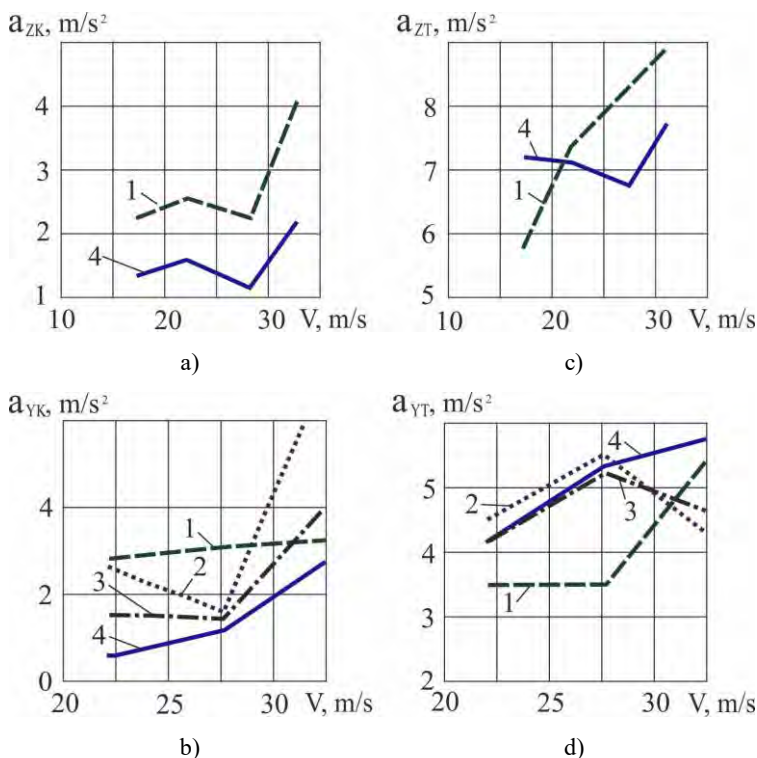


Fig. 11. Dependence of the change in maximum acceleration on the coasting speed of the locomotive; a) - vertical, b) - horizontal bodies in the area of the tie box, c) - vertical, d) - horizontal bogies, 1 - according to [67], 2 - model [83], 3 - model (8), 4 - model [18]

The results of solution to the problem of the locomotive's motion in traction mode on the site are set forth in Tables 6 and 7.

Table 6

**Values of the average total longitudinal adhesion forces [kN] on the track section at  $v=10$  m/s and  $v=20$  m/s, at maximum power, maximum at the adhesion characteristic 0.3**

Model	New profiles		Worn out	
	10 m/s	20 m/s	10 m/s	20 m/s
[81]	164.286	52.225	164.487	52.174
[83]	164.475	52.211	164.435	52.011
[18]	163.590	51.545	163.520	52.161

Table 7

**Values of the average total longitudinal adhesion forces [kN] on the track section at  $v=10$  m/s and maximum at the adhesion characteristic of 0.15 and  $v=20$  m/s and maximum at the adhesion characteristic of 0.1, at maximum power**

Model	New profiles		Worn out	
	10 m/s	20 m/s	10 m/s	20 m/s
[81]	164.390	52.262	164.480	52.192
[83]	164.360	52.233	164.405	52.169
[18]	157.550	49.520	156.960	49.169

The results of the traction parameters estimates when using different adhesion models differ to a greater extent than the dynamic ones. This is due to the fact that as a result of a different approach to solving the problem of the interaction of a locomotive wheel with a rail, the models take into account the factors influencing the adhesion process in different ways.

The values of the average total longitudinal adhesion forces along the section and the coefficient of use of adhesion weight under good contact conditions (clean, dry rails,  $\mu = 0.3$ ) for all models do not differ, (the value  $\eta = 0.941$  at  $v = 10$  m/s and  $\eta = 0.98$  at  $v = 20$  m/s) since they are the result of the action of the same tractive moments and the magnitudes of the forces  $F_{xsc}$  do not reach the adhesion limit (Table 7).

At the same time, the amplitude of changes in the adhesion force will be different for each specific model. Fig. 12, 13, 14 demonstrate the change in the vertical load and the adhesion force depending on the distance traveled for the first wheelset of the locomotive in traction mode and using different adhesion models. The oscillation amplitudes  $F_{sc}$  are observed in model [18]. For models [81, 83] the amplitudes of oscillation of the tractive force of one wheelset were 2-3 kN, for the adhesion model [18] - 5-6 kN, for the entire locomotive - 10-20 and 30-40 kN, respectively.

The amplitude of the change in the tractive force of the entire locomotive, according to [51], was 40-60 kN (Fig. 15). [64] provides the results of measuring the tractive force of one wheelset of an electric locomotive VL10a with an axial load of 24 tons when in traction mode (Fig. 16). The amplitude of fluctuations in the tractive force was 8-12 kN with coefficient of adhesion of 0.34-0.37. Comparison of these results shows that the results of the estimates using the adhesion model [18] are the closest to the experimental data in terms of the amplitude of oscillations of the tractive force.

Due to the biggest vibration amplitude, the smallest value of mean  $F_{sc}$  along the travel segment with deteriorating friction contact conditions is observed when using model [18] (Table. 7).

To this effect, at the maximum adhesion of 0.15,  $v = 10$  m/s,  $M_f = 14.5$  kNm per wheelset, the total average tractive force for the section in model [18] 4.6% or 7.5

kN smaller for the new wheel and rail profiles, and 4.2% or 6.85 kN for worn profiles than other adhesion models.

At maximum adhesion of 0.1,  $v=20$  m/s,  $M_r=4.5$  kNm per wheelset, the decrease in tractive force in model [18] was 5%, or 2.7 kN, for the new and 4.8%, or 2.5 kN, for worn profiles compared to models [81] and [83]

$\eta=0.941$  at  $v=10$  m/s for models [81, 83] and  $\eta=0.95$  for [18], at  $v=20$  m/s  $\eta=0.98$  for all models. Increase in the value  $\eta$  for model [18] is explained by the fact that the first (it is also the limiting) wheelset is at the adhesion limit, the level of decrease in its adhesion force is greater, and the adhesion coefficient is smaller than for the entire locomotive.

The results of the solution to the problem of locomotive movement in traction mode at maximum power at  $v=10$  m/s along the oil slick (i.e., a sharp decrease in frictional properties on the track section from  $\mu=0.3$  to  $\mu=0.1$ , followed by the recovery thereof) are shown in Fig. 17, 18.

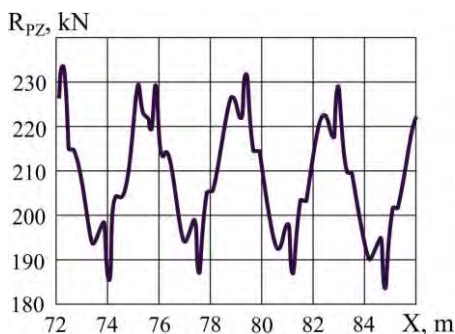


Fig. 12. Change in the vertical load from the first wheelset on the rails the speed of the locomotive  $v=10$  m/s

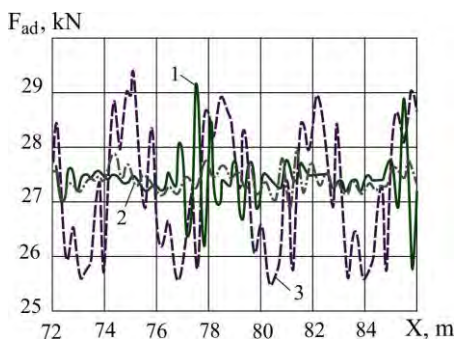


Fig. 13. Changes in the adhesion force of the first wheelset at the locomotive speed of  $v=10$  m/s and maximum adhesion  $\mu=0.3$ , - model [81], 2 - [83], 3 - [18]



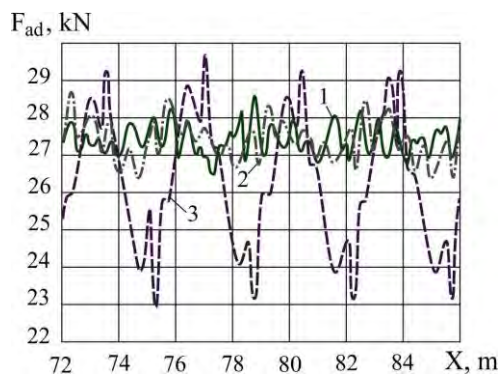


Fig. 14. Changes in the adhesion force of the first wheelset at the locomotive speed of  $v=10$  m/s and maximum adhesion  $\mu = 0.15$ , 1 - model [81], 2 - [83], 3 - [18]

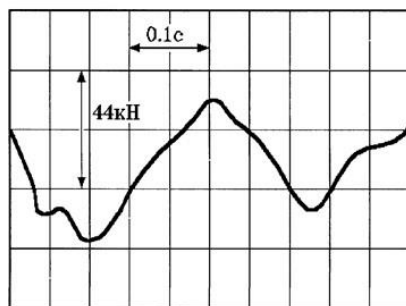


Fig. 15. Oscillograph chart of the tractive force of a locomotive with a support-axle drive [51]

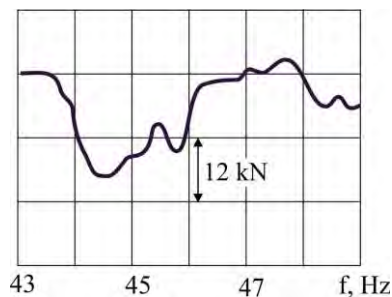


Fig. 16. Curve of the tractive force change from one axis of VL80a electric locomotive during the acceleration [78]

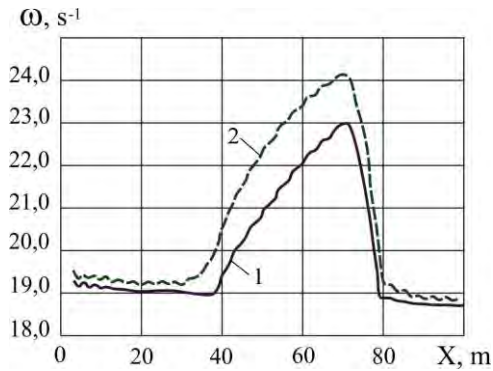


Fig. 17. Change in the angular speed of the first wheelset when the locomotive travels over an oil slick 30 m long (1 - for model [83], 2 - for model [18])

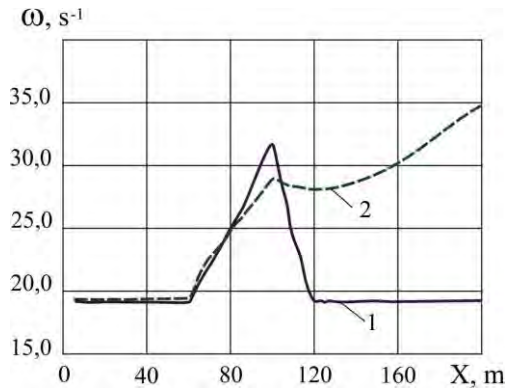


Fig. 18. Change in the angular speed of the first wheelset when the locomotive travels over an oil slick 50 m long (1 - for model [83], 2 - for model [18])

One can see that the estimates of the locomotive motion in different adhesion models are not the same.

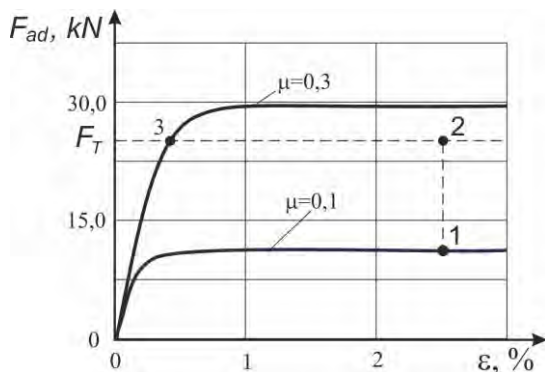
For a short slick ( $< 30$  m) passed over a relatively short time when no visible slipping occurs, the slipping stops for any model as soon as the frictional conditions are restored (Fig. 17).

In the event of a long-term presence of a locomotive on an oil slick (over 50 m long), when skidding develops over a long period of time, skidding does not stop when the frictional conditions are restored under model [18], but with model [83], the skidding does stop (Fig. 18).

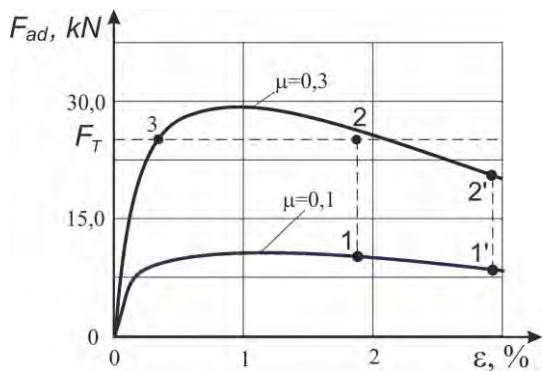
This is because there is no descending branch on the adhesion characteristic in model [83], and upon restoration of the frictional conditions of the contact, if the tractive force does not exceed the adhesion limit in the new conditions, a

decrease in the slip always occurs and the adhesion is restored (Fig. 19, a). Here, respectively, are the points: 1 - the moment of the end of the oil slick, 2 - restoration of frictional conditions ( $\mu = 0.3$ ), 3 - the end of the slipping process. In this case, when switching to a new adhesion characteristic ( $\mu = 0.3$ ) forces do not reach the limit (points 1, 2, 3).

According to model [18], the adhesion characteristics have a descending branch. Therefore, if the slipping process has developed deeply enough (Fig. 19, b, points 1', 2'), then the restoration of frictional conditions does not result in the cessation of slipping, because on the new traction characteristic ( $\mu = 0.3$ ) point 2' is still on the descending branch under skidding conditions and this process can be stopped only by dumping of the load, i.e. tractive forces, and this is exactly how they solve this problem in reality.



a)



b)

Fig. 19. The influence of the adhesion characteristics on the development of the slipping process (a) - model [83], b) - model [18])

If, with the improvement of frictional conditions on the new characteristic, the forces do not reach the adhesion limit (Fig. 19, b, points 1, 2, 3), the slipping can stop without load dropping.

When solving the problem of the starting of a locomotive with a train of carriages from standstill, a train of 20 carriages, 80 tons each, located on the site, was simulated. The resistance of the train of carriages when starting off and in the initial period of movement was determined in accordance with [3, 4]  $W_{tr}=42W/(29+s)$ , where  $s$  - the distance from the starting point, in km. When starting off, the limitation of the power of the locomotive by the current of the motors was simulated.

When using the model [18], the locomotive starts off at the maximum value of the adhesion making 0.375, which is quite consistent with real conditions.

For the adhesion model [83], unlike with the model [18], it was not possible to simulate the starting process. The breaking into slipping occurred even at the maximum adhesion of 0.6, which does not correspond to reality. This can be explained by the fact that at very low speeds, the longitudinal vibrations of the train set and the locomotive cause small, however considerably above the critical absolute values of the relative slip on the adhesion characteristic and the locomotive goes into slipping process. Therefore, as it follows from the review of the literature devoted to the study of the processes occurring during the operation of a locomotive in the traction mode, including slipping and starting, the authors use for calculations the experimental characteristics of adhesion [47, 60, 68] or introduce the "coefficient of angular stiffness of the elastic coupling of the wheel to the rail in the direction longitudinal to the axis of the track"[57], while theoretical models of adhesion are more often used to calculate the vehicle motion in coasting mode [10, 38, 50, etc.].

There is an obvious collision here, since the physics of the process of frictional interaction between the wheel and the rail does not depend on the mode of the locomotive motion, at least in the literature known to the author it is not indicated that the adhesion in the traction mode differs from the adhesion during the coasting. The adhesion process should be simulated in the same way in both traction and dynamic calculations.

According to the data obtained from solving the problem of starting a locomotive from standstill under poor frictional conditions of the wheel-rail contact ( $\mu = 0.2$ ), the locomotive went into slipping. At the same time, the process of development of frictional self-oscillations of the wheelset axle at 30-35 Hz was observed (Fig. 20). The value of the dynamic moment on the traction motor shaft was 4.73 kNm with traction moment before the commencement of slipping 8.11 kNm.

Similar processes were recorded when testing the operation of the 2TE121 diesel locomotive (Fig. 21) and the VL81, ChS4 electric locomotives in the starting mode under poor frictional conditions and the development of the slipping process [30, 32, 31, 47, 57].

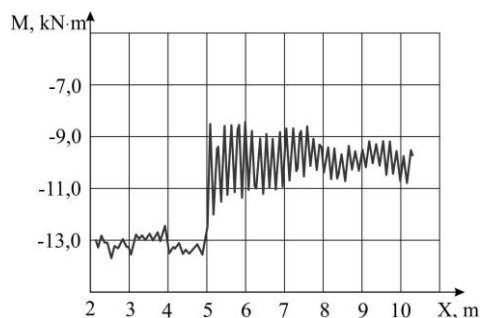


Fig. 20. Moment on the axle of a wheelset of a locomotive (calculation)

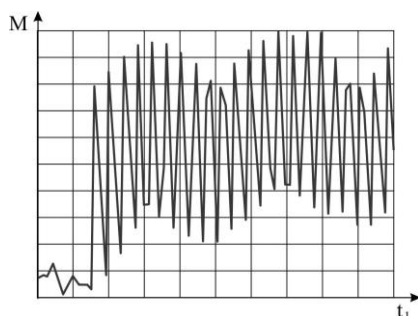


Fig. 21. Moment on the axle of a wheelset of a 2TE121 diesel locomotive [30.57]

In [31, 32], when testing a TEP10 diesel locomotive No. 333 in the slipping mode at the start from standstill, the slipping was obtained with the development of oscillatory processes. In this case, the value of the dynamic moment on the traction motor shaft was 4.15 kN·m with the traction moment before the slipping occurred of 8.65 kN·m.

The comparison of these results once again confirms the reliability of the developed model.

## 6.2. Influence of the tractive force of a locomotive on the results of calculations of dynamic processes in the "vehicle-track" system

To assess the influence of the traction moment and frictional conditions of the wheel-to-rail contact on the dynamics of the locomotive's motion, a series of calculations was carried out for two traveling speeds: at  $v=10$  m/s,  $\mu$  was taken equal to 0.3 and 0.15; at  $v=20$  m/s,  $\mu$  was taken equal to 0.3 and 0.1. Minimum values  $\mu$  are taken from calculating the adhesion force close to the adhesion limit, but not exceeding it.

Mathematical expectations of the maximum frame, lateral and transversal adhesion forces for combinations of the new wheel profiles with worn-out rails and worn-out wheels with worn-out rails are set forth in Tables 8, 9 and in Figs. 22, 23.

Table 8

**Estimates of the mathematical expectations of the maximum frame, lateral and transversal adhesion forces (calculation) for the new wheel and rail profiles [kN]**

Wheelset number										
			1	3	4	6	1	3	4	6
$v, \text{ m/s}$	$\mu$	Traction				Coasting				
10	0.3	$R_{by}$	3.87	6.08	8.35	9.32	5.23	3.07	8.42	9.33
		$F_y$	9.93	4.28	9.45	6.81	9.82	2.25	6.98	7.48
		$R_{py}$	21.81	14.42	18.60	16.53	18.43	7.46	11.87	9.00
10	0.15	$R_{by}$	12.40	11.84	12.26	19.64	6.86	2.46	5.68	7.00
		$F_y$	2.27	2.27	2.60	3.22	2.26	1.45	2.62	2.49
		$R_{py}$	21.00	14.90	36.32	37.87	11.82	9.09	11.34	22.18
20	0.3	$R_{by}$	12.59	12.79	13.39	17.76	12.37	13.23	14.05	18.42
		$F_y$	13.51	10.34	16.29	13.02	11.01	10.01	14.58	13.05
		$R_{py}$	43.53	36.66	37.10	32.38	32.83	37.90	35.27	36.81
20	0.1	$R_{by}$	15.96	17.15	15.68	18.53	14.03	15.83	15.20	18.47
		$F_y$	2.15	2.70	2.89	3.22	2.26	3.34	2.95	3.66
		$R_{py}$	55.47	47.47	55.05	48.74	40.94	47.95	40.80	45.72

Table 9

**Estimates of the mathematical expectations of the maximum frame, lateral and transversal adhesion forces (calculation) for worn-out wheel and rail profiles**

Wheelset number										
			1	3	4	6	1	3	4	6
$v, \text{ m/s}$	$\mu$	Traction				Coasting				
10	0.3	$R_{by}$	7.68	6.64	6.76	11.23	8.80	7.67	8.74	9.50
		$F_y$	10.23	4.47	8.51	8.84	7.58	5.91	7.00	7.25
		$R_{py}$	25.49	7.96	18.52	17.53	9.76	9.18	9.19	8.72
10	0.15	$R_{by}$	14.63	10.68	16.71	22.35	4.40	3.70	4.94	5.88
		$F_y$	2.70	2.72	3.90	5.13	1.48	1.37	2.02	4.52
		$R_{py}$	28.74	19.94	34.92	51.44	9.40	6.71	7.74	19.31
20	0.3	$R_{by}$	12.76	16.38	15.11	21.13	14.64	16.69	16.74	20.00
		$F_y$	17.05	14.85	15.78	19.39	15.06	15.22	14.89	18.52
		$R_{py}$	47.59	42.06	46.62	31.59	47.73	37.88	42.56	49.19
20	0.1	$R_{by}$	13.85	12.86	17.61	17.81	15.11	16.19	15.43	19.56
		$F_y$	4.03	2.48	3.46	4.25	3.65	5.59	4.27	6.10
		$R_{py}$	23.33	35.29	53.31	41.99	47.73	42.44	41.68	56.65

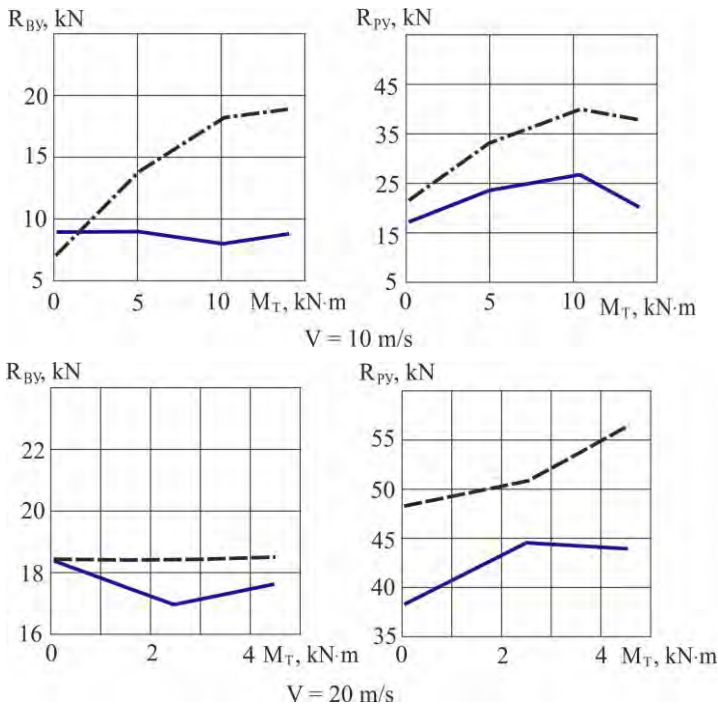


Fig. 22. Changes in the maximum frame and lateral forces depending on the tractive moment for new wheel and rail profiles —  $\mu = 0.3$ ; — · —  $\mu = 0.1$ ; - - -  $\mu = 0.15$

As one can see from Tables 8, 9 and Figs. 22, 23, in most of the calculated modes of motion, when traction is applied to the wheelset, an increase in the maximum values of frame (2.8) and lateral (1.7 times) forces is observed.

This effect does not appear when the adhesion force does not reach the maximum possible value determined by the frictional conditions.

For example, at  $v = 10$  m/s,  $R_{by}$  and  $R_{py}$  increase much greater than at  $v = 20$  m/s. This is due to the fact that  $M_t$  at  $v = 10$  m/s equals 14-14.5 kNm per wheelset, versus 4-4.5 kNm at  $v = 20$  m/s. At  $v = 20$  m/s, for worn out profiles of wheels and rails, no increase in  $R_{by}$  and  $R_{py}$  is observed.

To combine the new wheel profiles with the new rails at  $v = 10$  m/s and  $\mu = 0.3$  with an increase in  $M_t$  from 0 to 14.5 kNm per wheelset, the maximum frame forces change little, lateral forces increase by 45%, with  $\mu = 0.15$  the maximum frame forces increase by 170%, lateral forces - by 80%. For worn wheels and rails at the same travel speed at  $\mu = 0.3$ , frame forces increase by 18%, lateral forces - by 160%. At  $\mu = 0.15$ , the frame forces increase by 280%, lateral forces - 170%.

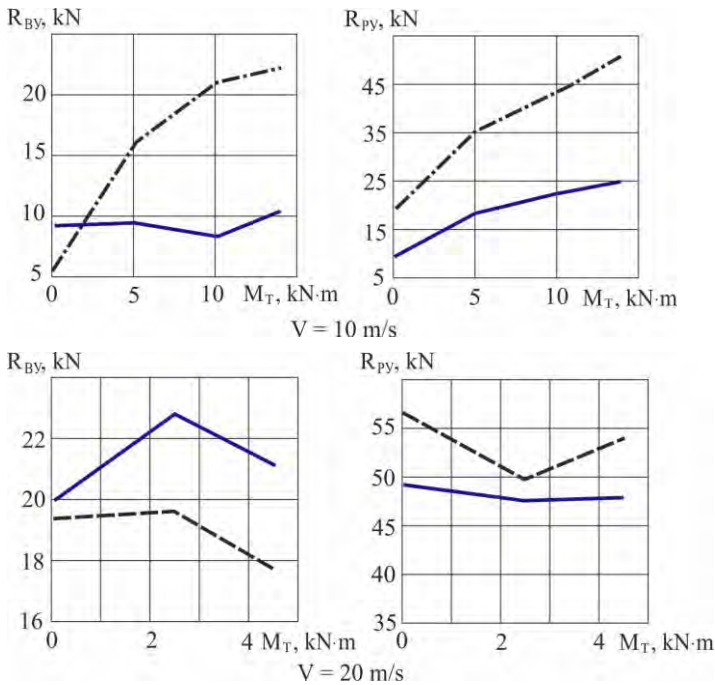


Fig. 23. Changes in the maximum frame and lateral forces depending on the tractive moment for worn wheel and rail profiles —  $\mu = 0.3$ ; — · —  $\mu = 0.1$ ; - - -  $\mu = 0.15$

The level of frame and lateral forces in the traction mode at  $v = 10 \text{ m/s}$ , especially for worn out profiles of wheels and rails, is comparable to the level  $R_{by}$  and  $R_{py}$  at  $v = 20 \text{ m/s}$ .

A similar effect of the increase in  $R_{py}$  (by 140%) occurs when the frictional conditions deteriorate in the coasting mode and, to an even greater extent, in the traction mode (an increase in  $R_{by}$  reaches 110% and  $R_{py}$  - 100%).

At  $v = 10 \text{ m/s}$ ,  $M_t = 14.5 \text{ kNm}$  and a decrease  $\mu$  from 0.3 to 0.15 for the combination of the new wheel profiles with the new rails, the maximum values of frame forces grow by 110%, lateral forces - by 70%, for worn wheels and rails, frame forces increase by 100%, and lateral forces - also by 100%.

At  $v = 20 \text{ m/s}$ ,  $M_t = 4.5 \text{ kNm}$  and a decrease  $\mu$  from 0.3 to 0.1 for new profiles of wheels and rails, an increase in frame forces does not occur, lateral forces increased by 27%, for worn wheels and rails the increase in frame forces was 19%, for lateral forces - 12%.

According to the analysis of the results of the locomotive's motion calculations, there is a significant influence of the tractive force and frictional



conditions in the contact between the wheel and the rail on the dynamic processes in the transverse direction (Tables 8, 9, Fig. 22, 23).

These results have been further confirmed experimentally. Destabilizing effect of the traction torque on the locomotive motion in the horizontal plane was registered in experimental work carried out at the Department of Locomotive Engineering of the East Ukrainian State University and during the test runs of the TEM2 locomotive No. 7024 by the All-Russian Research Diesel Locomotive Institute [14, 15, 43].

The results herein are of considerable interest in determining the dynamic qualities of a locomotive, since the tractive force can have a noticeable destabilizing effect on the process of its movement.

Let us compare these data with the results of other studies on the influence of the traction moment on the rail vehicle movement.

In [14, 15, 33, 39, 44, 55, 56], the effect of the traction moment on the nature of the locomotive motion or its wheelset is noted. However, opinions on the influence of the latter are divided. For example, the traction moment allegedly stabilizes the movement of the vehicle in the straight section of the track in [39], while destabilizing the same in [14, 19, 33, 43, 44].

Let us try to sort this out.

The locomotive motion and generation of the tractive force occurs by way of the wheelsets rolling on a railway track. Therefore, we should consider the results of calculating the single wheelset motion in the stopping and the traction modes [20]. In addition, this approach makes the task easier, since the wheelset-track system is much simpler than the locomotive-track system.

The wheelset interacts with the railway track in the horizontal plane by means of adhesion forces in the contact between the wheel and the rail, inertia, gravitational stiffness and the interaction of the wheel flange with the rail head at the moment of their contact (Fig. 24). Their action determines the nature of the wheelset motion.

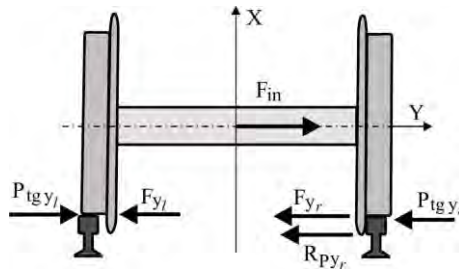


Fig. 24. Diagram of the interaction forces of a wheelset with the railway track

The adhesion force is the response of the rail to the external influences and is by its nature a friction force [41], i.e. the response of resistance to the movement of the contacting bodies. This kind of movement (sliding) is the result of the traction moment and the kinematics of the wheelset motion:

$$\vec{F}_{ad} = \vec{F}_m + \vec{F}_\kappa$$

where  $\vec{F}_m$  - the component of the adhesion force caused by the traction moment;

$\vec{F}_\kappa$  - kinematics of the movement (wobbling).

$\vec{F}_{ad}$  - broken down into longitudinal and transverse components. At first approximation, one can record (1)

$$F_{ad} = \sqrt{F_{adx}^2 + F_{ady}^2} . \quad (1)$$

$F_m$  - can also be broken down into longitudinal and transverse components (fig. 25).

$F_{tx}$  - performs the useful work of moving the wheelset in the longitudinal direction.

$F_{ty}$  - always directed along the wobble angle ( $F_{ty} = F_t \sin \varphi$ ) and destabilizes the motion, since it acts in phase with the transverse speed of motion ( $\varphi$  and  $\vec{F}_{ad} = \vec{F}_m + \vec{F}_\kappa$  change in one phase). Therefore, a slight (1-2%) decrease in  $L$  is observed with an increase in  $M_t$  (ranging from 0 to 1025 kNm) [18].

With a further increase in  $M_t$ ,  $L$  begins to increase. This is due to the effect of mutual influence of  $F_{scx}$  on  $F_{scy}$  and it happens as follows.

With the growth of  $M_t$ ,  $F_{stx}$  increases because  $M_t$  is always located in the vertical plane oriented in the direction of the wheelset motion. Things are more complicated with  $F_{scy}$ . From (1) it follows

$$F_{ady} = \sqrt{F_{ad}^2 - F_{adx}^2}$$

Under certain conditions,  $F_{ad}$  can be considered constant, so  $F_{ady}$  decreases with the increasing  $F_{adx}$ .

In addition, due to the nonlinear nature of the adhesion, an increase in the adhesion force by the same amount but in different parts will cause an uneven (increasing) growth in  $\varepsilon$ . Then to generate the same  $F_{ady}$  with an increase in tractive torque, one would need more  $\varepsilon_y$  (Fig. 26,  $F_{ady1} = F_{ady2}$ ,  $\varepsilon_{y1} < \varepsilon_{y2}$ ). Consequently, while increasing  $F_{adx}$ ,  $M_t$  will also increase the value of transverse sliding that is necessary for maintaining  $F_{ady}$ .

Therefore, with an increase in the tractive moment, there is a decrease in the transverse forces of adhesion and, consequently, in the forces of resistance to the transverse motion. As a result, lateral forces increase (up to 90% depending on the speed and magnitude of  $M_t$ ), same as the rails displacement (100%) and the time of contact with the ridge of the rail head wheel (80%) for new profiles of wheels and rails. The wavelength of the wobble drops at first [18] and then increases due to a significant reduction in  $F_{ady}$  and the increasing time of contact between the ridge and the rail [18], i. e. lateral adhesion forces can no longer keep the wheelset in the track.

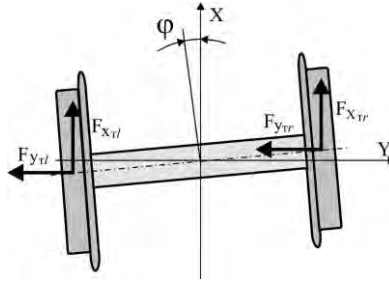


Fig. 25. Pattern of the action of tractive forces on the wheelset

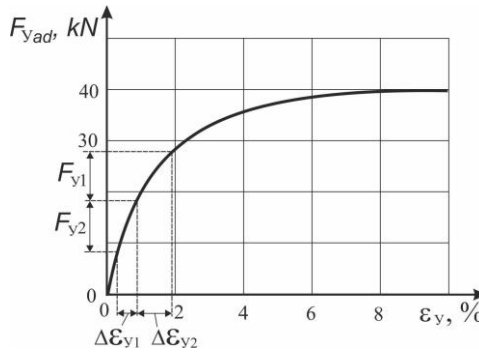


Fig. 26. Influence of the changing adhesion force on the values of transverse skid

For worn profiles, the increase in the wobble wavelength [18] is observed at the  $M_t$  lower than for the new profiles. This is due to the fact that the wobble frequency, the transverse speed of the wheelset in the railway track, and, consequently, the value of  $F_{ady}$  in this case, is larger (for example, at  $v = 10$  m/s, the amplitude of changes in  $F_{adx}$  is 8.1 versus 1.52 kN for the new wheel and rail profiles) and the influence of  $F_{adx}$  on  $F_{scy}$  occurs at a lower  $M_t$ . The movement of

the wheelset is largely determined by the forces of gravitational stiffness, which in this case are greater than for the new profiles (their amplitude is 12.02 against 0.084 kN).

Experimentally [14, 15, 13, 44, 80, 84] (Fig. 27), the influence of  $F_x$  on  $F_y$  and  $\varepsilon_x$  on  $\varepsilon_y$  was established.

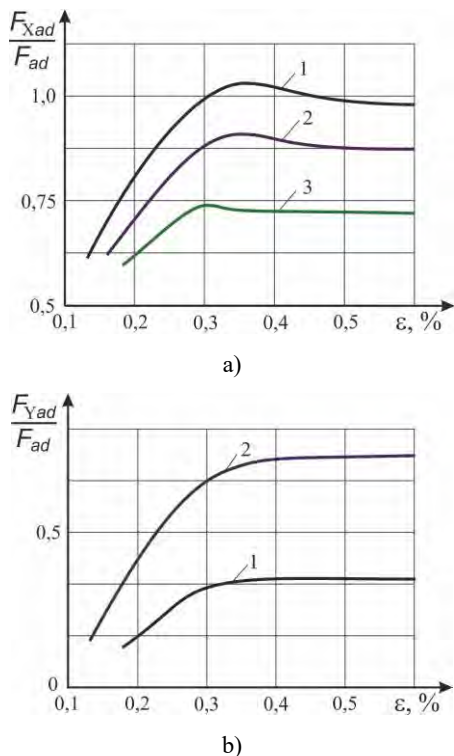


Fig. 27. The influence of the values of longitudinal and transverse skid on the adhesion properties; a) - dependence of the relative adhesion force on the longitudinal skid at varying values of the transverse skid: 1 -  $\varepsilon_y/\varepsilon_x = 0$ ; 2 -  $\varepsilon_y/\varepsilon_x = 0.5$ ;  $\varepsilon_y/\varepsilon_x = 1$ ; b) - the dependence of the relative transverse force on the longitudinal skid at varying values of the transverse skid:

1 -  $E_y/E_x = 0.5$ ;  $E_y/E_x = 1$

The movement of a locomotive in traction and coasting modes gives the same qualitative picture as the calculations of the movement of a single wheelset, but there are some peculiarities. The first feature is associated with the action of the transverse components of the tractive force. The wobble angles of a wheelset in a

carriage are smaller than that of a single one. Therefore, the values of  $F_{ty}$  (Fig. 25) are small and have no noticeable impact on the locomotive motion. The second feature is the presence of disturbances coming from the track in both the vertical and horizontal planes. Their impact appears to be as follows.  $M_r$  increases  $F_{adh}$  and decreases  $F_{ady}$ , i.e. the forces of resistance to displacement in the transverse direction, therefore, the kinetic energy of the movement of the elements of the "wheel-rail" system in this direction caused by the perturbations is dampened at a smaller extent. This also increases the contact time of the wheel flange with the rail head. And the longer the ridge is in contact with the rail, the more disturbances from the track will be transmitted to the vehicle in the horizontal plane. In addition, at the moment of contact of the flange with the rail head, when choosing a clearance in the track, the nature of the interaction between the wheel and the rail changes. It is carried out not only by means of  $F_{ad}$  but also by the elastic forces of the rail length, the stiffness of which is very high, which at this moment causes an increase in the interaction forces in the "vehicle-track" system.

The tractive force, due to its influence on  $F_{ady}$ , can cause a significantly intensify the dynamic processes.

The following patterns be observed in the calculation results.

1. Depending on the magnitude of the tractive force and frictional conditions,  $M_t$  may have a considerable destabilizing effect on the nature of the locomotive motion, since it causes an increase in the dynamic forces (frame forces by 180-280% max, and lateral forces - by 80-170%).
2. Deterioration of the frictional conditions has the same effect on the processes occurring during the locomotive motion, as does the increase in the tractive torque.
3. The wear of the profile of the wheel rim causes an increase in dynamic forces during the movement of the vehicle. In most of the calculated driving modes, frame and lateral forces for worn wheels are 40-70% higher than for the new ones.

### **6.3. Influence of dynamic processes on generation of the tractive force during the locomotive motion**

A lot of works indicate that the dynamic processes occurring during the locomotive motion have a significant impact on generation of the tractive force [14, 15, 21, 22, 47, 51, etc.].

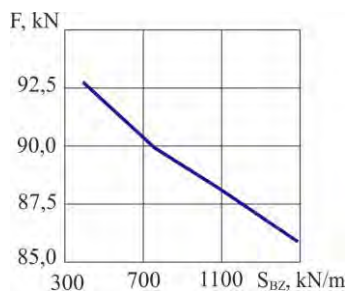
[47, 51] show the dependence of the average tractive force generated by a locomotive without going into the slipping on a track section on the type and amplitudes of vertical disturbances. No similar assessment of the influence of horizontal disturbances on the magnitude of the tractive force is available.

Therefore, this work involved calculations and estimates of the influence of oscillations in both the vertical and horizontal planes on the traction of the locomotive.

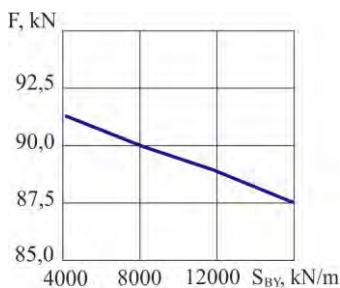
To simplify the task, the extent of the tractive force was estimated depending on the stiffness of the axle-box stage of the spring suspension in the vertical and horizontal directions, since the level of dynamic forces in the locomotive directly depends on the stiffness of the spring suspension elements.

Calculations were carried out for one section of a 2TE116 diesel locomotive moving in the traction mode at  $v = 10$  m/s and  $\mu = 0.1$ . Vertical stiffness of the axle-box stage  $S_{bz}$  varied from 377 to 1508 kN/m, the transverse ( $S_b$ ) - from 4000 to 16000 kN/m per axle unit.

The results of calculations of the tractive force averaged over the section of the track, generated by the locomotive without going into skid, and the dynamic forces in the "locomotive-track" system are provided in Fig. 28, 29, 30.



a)



b)

Fig. 28. Change in the average tractive force in the area depending on a) - the vertical stiffness of the axle-box spring suspension; b) - transverse stiffness of the axle-box spring suspension

As one can see from Fig. 28, 29, 30, the increase in  $S_{bz}$  caused the increase of maximal vertical dynamic forces in the axle-box spring suspension by 54.6%, and from wheelsets to track - 55.5%.  $R_{by}$  and  $R_{ry}$  decreased by 35.1 and 41.2%, respectively. The average tractive force decreased by 7.67%.

The increase in  $S_{by}$  led to the increase in frame and lateral forces by 100 and 13.15%, respectively, while the average tractive force decreased by 4.52%. The values of the maximum vertical dynamic forces remained practically unchanged.

The calculation results show that the dynamic processes occurring during the locomotive motion have a significant impact on generation of the tractive force.

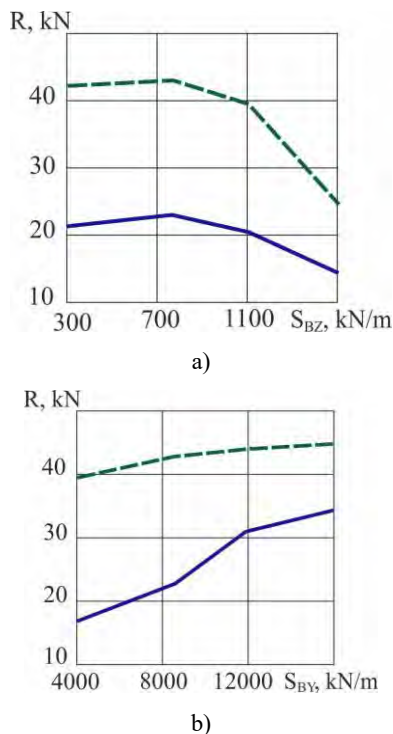
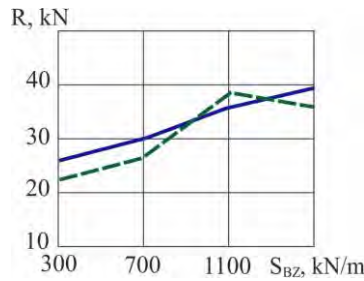
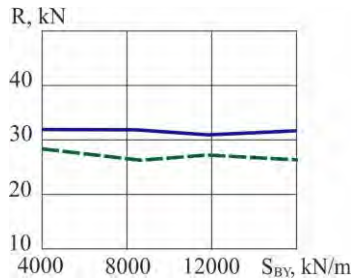


Fig. 29. Change in the maximum dynamic forces in the "locomotive-track" system depending on a) – the vertical stiffness of the axle box spring suspension; b) – the transverse stiffness of the axle box spring suspension



a)



b)

Fig. 30. Change in the maximum dynamic forces in the "locomotive-track" system depending on a) - the vertical stiffness of the axle box spring suspension; b) – the transverse stiffness of the axle box spring suspension; ———  $R_{hz}$ , - - -  $R_{rz}$  redistribution of vertical loads on wheelsets during traction and braking in order to align them [22, 29, 51];

#### 6.4. Analysis of the principles of operation of devices that improve the adhesion of the wheels of the locomotive to the rails in traction and braking modes

From the analysis of the literature, various methods are known to improve the adhesion of the wheels to the rails when the locomotive is moving in traction and in braking modes. Let us highlight the most common ones:

- redistribution of traction (braking) forces across the wheelsets in a locomotive depending on the vertical loads or sliding [22, 29, 54, 85];
- the use of traction electric motors with more rigid characteristics, including asynchronous ones, [60, 65], Fig. 31;

the use of devices for feeding the abrasive materials into the contact of the wheel with the rail (sandboxes).



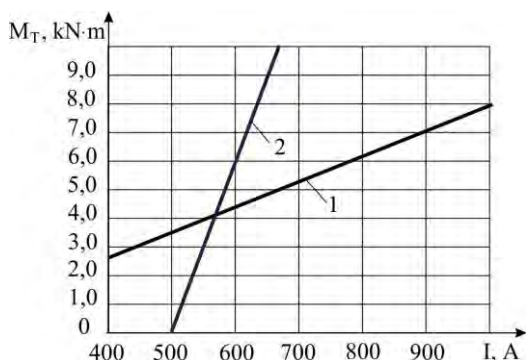


Fig. 31. Dependence of the torque of the traction motor on the current strength; 1 - conventional traction electric motor, 2 - with more rigid characteristics

The author has developed some design solutions that improve the conditions for the generation of traction and braking forces of the locomotive, based on the principles of redistribution of tractive moments on the wheelsets and the vertical loads, and the use of sandboxes, for which applications for inventions have been submitted and a positive decision [71] and copyright certificates [58, 59, 69, 70, 74] have been received.

This section is devoted to assessment of the effectiveness of design solutions [69, 59, 58, 70, 71, 74] using the mathematical locomotive motion model developed by the author.

"A device for adjustment of electric traction motors of a vehicle" [71] is designed for adjustment of traction torques by redistributing the currents between the motor circuits in order to reduce the torque on the motors that are in the worst adhesion conditions and to increase the tractive torque on the motors with the wheelsets in better adhesion conditions.

The design of the device comes in two versions. One of them is shown on Fig. 32. The device comprises traction motors 1 and 2, current transformers 3 and 4, a power supply unit containing a transformer 5, a differential transformer 6, a rectifier bridge 7, a coil 8, an adjustment resistor 9, a potentiometer 10, and a movable core contact 11.

The device operates as follows.

The power is supplied through transformer 5 to the windings of current transformers 3 and 4. In the event of equal wheelset rotation speeds, the currents flowing through the power circuits of the motors are equal. Accordingly, the currents flowing through the windings of transformers 3 and 4 are equal. In this case, currents of the same potential are supplied to the input of the differential transformer 6 (to its primary opposing windings), so the voltage at the output of its secondary winding is zero. There is no voltage on the electromagnetic coil 8, the

contact-core 11 is in the zero position and the resistance in the circuits of motors 1 and 2 is the same.

If the rotation speeds in the wheelsets are different, the equality of currents in the power circuits of traction motors 1 and 2 is disrupted. For example, on wheelset 1, which is more prone to slipping, there was an increase in  $\varepsilon$ . Accordingly, the current in the power circuit of motor 1 also decreases in the winding of transformer 3. The balance of the currents flowing through the primary windings of the differential transformer 6 is disrupted. An EMF will appear in its secondary winding, the value of which is proportional to the difference between the currents of motor 1 and motor 2.

The voltage of transformer 6 goes through the rectifier bridge 7 to the terminals of coil 8. In this case, the contact-core 11 is drawn into the coil, changing the resistance in the circuits of traction motors 1 and 2 in such a way that in the circuit of motor 1 the resistance increases, and in the circuit of motor 2 it decreases. The currents and, consequently, the torques are redistributed.

By increasing the resistance in the circuit of motor 1, we reduce the torque on the wheelset, which is in the worst conditions in terms of adhesion and the wheel skid of which is higher, and, conversely, by reducing the resistance in the circuit of motor 2, we increase the tractive moment of the wheelset, which is in the best adhesion conditions. This helps maintain the total tractive effort of the locomotive while reducing the tendency to slipping.

The second version of the device is presented in Fig. 33. It includes traction motors 1 and 2, current equalizer 3 that controls a movable contact of potentiometer 4, which is located in the control circuit of pulse thyristor converters 5 and 6, and resistor 7. Control circuits of thyristor converters 5 and 6 contain linear amplifiers 8, converters 9, nonlinear amplifiers 10 and pulse shapers 11.

The device works as follows. In the event of an increased skid on one of the wheelsets, for example, wheelset 1, the current in the circuit of the motor 1 would decrease. Contact 4 of current equalizer 3 closes the control circuits of thyristors 5 and 6.

Potentiometer 4 adjusts the voltage between the control circuits of thyristor converters 5 and 6. The drive of the movable contact of the potentiometer can be designed in a similar way described in the first version of the device.

In this case, the values of the output pulses of pulse shapers 11 will be proportional to the voltage in the control circuits of thyristor converters 5 and 6. Thyristor in the circuit of motor 1 will receive longer pulses and most of the current in the motor circuit will go through resistor 7.

Thyristor in the circuit of motor 2 receives signals of shorter duration and, therefore, a smaller part of the current in the motor circuit will go through resistor 7.

This will reduce the current in the circuit of motor 1 and increase it in the circuit of motor 2. Traction moments will be redistributed in a similar way.

Inventor's certificates No. 1799769 and No. 1675144 for the invention of devices that improve the conditions of locomotive adhesion during the braking are based on the principle of redistribution of vertical loads over the wheelsets [69, 70].

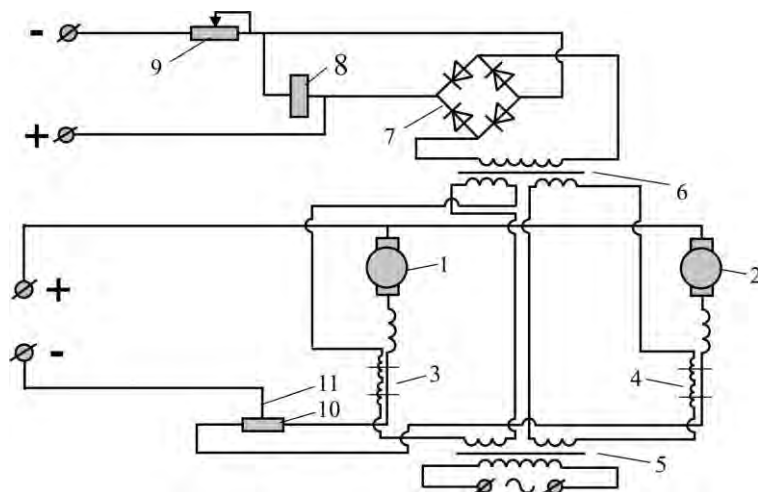


Fig. 32. Vehicle traction motor control device (option 1)

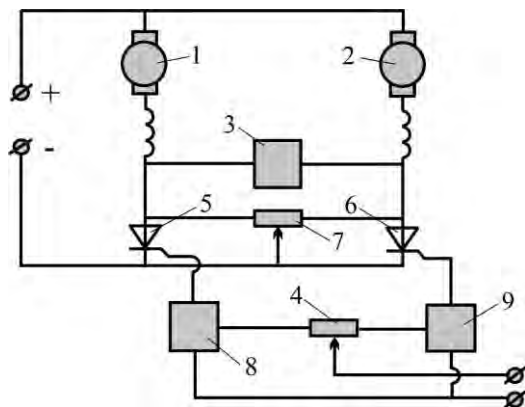


Fig. 33. Vehicle traction motor control device (option 2)

The principle of operation of both devices is as follows. Brake pads on the wheels of the locomotive are installed at a certain angle. As a result, when the

braking force presses the pads against the wheel, a vertical component of this force arises, which contributes to redistribution of vertical loads over the wheelsets in the locomotive (Fig. 34). The difference in vertical loads depends on the magnitude of the braking force; therefore, its vertical component will add or take the load off the wheelset, depending on redistribution of the vertical loads in the locomotive during the braking.

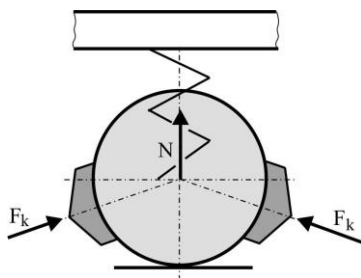


Fig. 34. Diagram of the action of forces with brake pads installed at an angle to the horizontal plane

Two versions of the device are suggested. The first one requires the installation of brake pads at an angle on the middle wheelset in a three-axle locomotive bogie (Fig. 35). In this case, the vertical component of the braking force will unload the middle wheelset and add the load to the extreme ones. In the process of the locomotive braking, the first wheelset in the direction of travel is the most loaded, and the load on the last one is the smallest, i.e. limiting by adhesion. As a result, the loads on the third and second wheelsets will be equalized. Additional load goes onto the third wheelset in the bogie (the last in the locomotive), its adhesion conditions are thereby improved.

In the second version of the device, the brake pads are installed at an angle on the extreme wheelsets in the bogie in a way so as to take the load off the first wheelset in the direction of the travel and carry the load over onto the last one (Fig. 36). As a result, the vertical loads are equalized across all wheelsets in the bogie.

Inventor's certificates No. 1770188, 1781112 and 1801827 for the inventions were obtained on applications for the locomotive sandbox designs [59, 58, 70].

Sandbox in Inventor's certificate No. 1801827 is designed to improve the performance by managing the productivity. In Inventor's certificate No. 1770188, sandbox operation is improved by preventing the caking of bulk materials. Inventor's certificate No. 1781112 is dedicated to sandbox performance control.

The developed mathematical locomotive motion model makes it possible to analyze the efficiency of the above methods aiming to improve the adhesion conditions and to assess their influence on traction and braking.

To assess the effect of using the device [71], the following locomotive designs were modeled when moving in the traction mode - the initial one; with the device

described above, redistributing the traction moments over the wheelsets, set to change the resistance in the motor circuit by 0.0002 Ohm for every 1 A of the difference in current strength. It also assesses the effect of the use of traction motors with more stringent characteristics, simulating a locomotive with traction electric motors that have a more rigid dependence of the torque on the speed of motion (current strength) (Fig. 36).

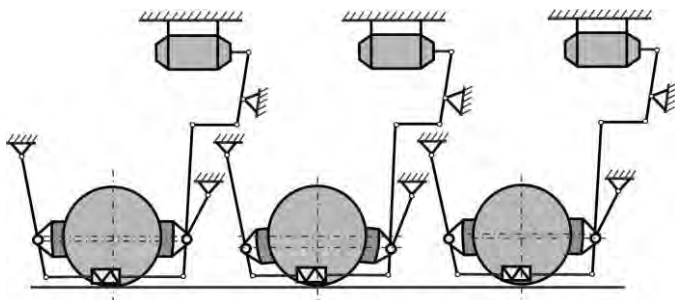


Fig. 35. Brake gear

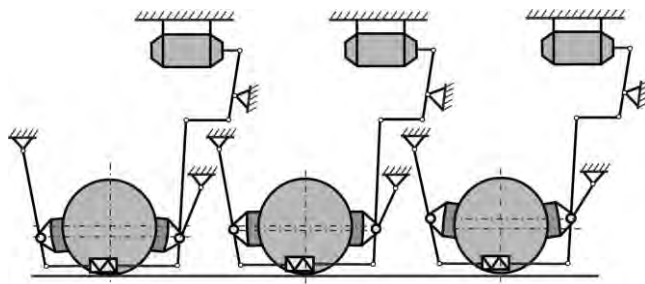


Fig. 36. Brake gear

The following tasks were considered:

- locomotive motion in traction mode on the site at  $\mu = 0.3$ ;
- the locomotive travel in traction mode at  $v = 10$  m/s on the oil slick ( $\mu$  drops from 0.4 to 0.2).

The task of starting off was not considered, because starting off at maximum power, the motors operate under conditions when the current is limited and there is no effect from the use of the traction motors with more stringent characteristics and the traction torque control device.

Calculation results  $\eta$  obtained by solving the first problem for all three versions of locomotive models are set forth in Fig. 37.

As one can see, during the motion, when the limitation on the magnitude of the motor current does not apply, the redistribution of the traction moments and

the use of electric motors with the more rigid characteristics give a significant effect on increasing  $\eta$ . At  $v=5$  m/s and using the device [71]  $\eta$  would increase by 5.4%; the use of motors with rigid characteristics would increase  $\eta$  by 4%.

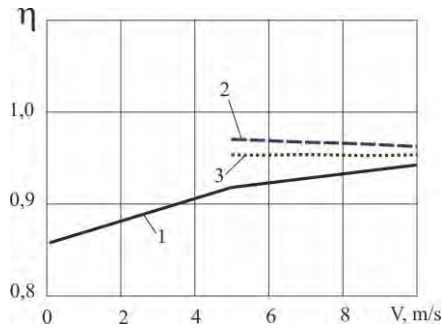


Fig. 37. The change in  $\eta$  depending on the locomotive speed in traction mode at maximum power; 1 - the original version, 2 - with the redistribution of traction moments, 3 - when using traction electric motor with more rigid characteristics on the middle wheelset in the bogie

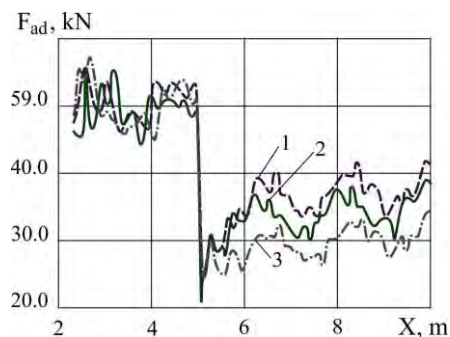
The results of solution to the problem of a locomotive hitting an oil slick in traction mode are set forth in Fig. 38 and Fig. 39. Here you will also find the results of calculations for a locomotive using the traction motors with more stringent characteristics.

A locomotive with conventional electric motors of sequential excitation immediately goes into slipping, the current and tractive torque drop, but not enough to stop the slipping (Fig. 38, 39).

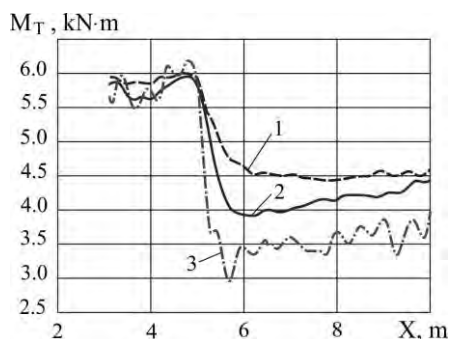
When a locomotive equipped with a device that redistributes tractive moments over the wheelsets [71] hits an oil slick,  $F_{ad}$  drops, the rotation speed of the wheelset goes up, but in this case  $M_t$  is reduced by a larger amount than in the original version, and the locomotive avoids any further slipping (Fig. 38, 39).

A similar scenario was obtained for locomotive equipped with traction motors with more stringent characteristics (Fig. 38, 39).

The results in Fig. 39 and 40 are in good agreement with the results obtained experimentally and theoretically [29, 54, 60, 65]. According to experimental measurements of the adhesion coefficient on electric and diesel locomotives of the German Railways [90], the maximum adhesion coefficient of rolling stock is 0.30-0.33, but some locomotives with traction motors having more rigid characteristics and a perfect traction motor control system are consistently demonstrating the higher values of the coefficient of adhesion. For example, the E120 electric locomotive with asynchronous traction motors has a friction coefficient of 0.419. Similar data on electric locomotives E1200, VL80<sup>a</sup> and VL86<sup>f</sup> with asynchronous traction motors are set forth in [78].



a)



b)

Fig. 38. Development of slipping on the first wheelset when hitting an oil slick; a - change in the adhesion force, b - change in the electric motor; 1 - initial version, 2 - electric motor with more stringent characteristics; 3 - with redistribution of the traction moments

It is also noted in [64] that the use of independent excitation on electric locomotives, i.e. motors with more rigid characteristics, electric pairing of the axles and uneven excitation damping along the bogies, meaning the redistribution of tractive effort, improves the adhesion of wheels to rails, reduces the slipping and the extent of wear of the locomotive rims.

The obtained results confirm an increase in  $\eta$  and a decrease in the tendency to slipping in the limiting wheelset when using the developed traction torque control device in the wheelsets of the locomotive [71].

Now let us consider the operation of devices [69, 70] that improve the conditions for generation of the braking power of the locomotive.

To analyze the results of these methods of improving conditions during braking, calculations were made for single locomotive motion in the braking mode, in which the original version of the locomotive was considered with device [69] and device [70].

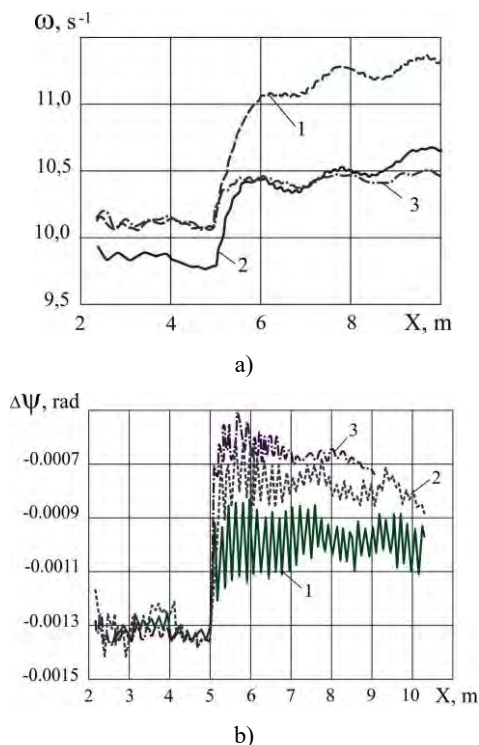


Fig. 39. Development of slipping on the first wheelset when hitting an oil slick; a - change in the angular speed of the wheel, b - the development of auto-frictional vibrations (angle of rotation of the axis); 1 - initial version, 2 - electric motor with more stringent characteristics; 3 - with redistribution of the traction moments

In this case,  $\eta$  characterizes the tendency of the locomotive to slip in the limiting wheelset. There is a significant increase in  $\eta$  with redistribution of vertical loads. At  $v=5$  m/s, the increase  $\eta$  was 4% and 8.5%, at  $v=10$  m/s,  $\eta$  increased by 2.2% and 4.5% for the first and the second versions of the device respectively.

As it follows from the calculation results hereinabove, the use of the developed devices [69, 70] will reduce the tendency of the locomotive to slip in the limiting wheelset.

Let us analyze the performance of the sandbox [58, 59, 74].

The initial version of the locomotive was also considered with the use of a sandbox. The ingress of sand into the contact of the wheel with the rail causes an increase in the maximum on the traction characteristic and was modeled with  $\eta = 0.4$ .

The calculation results obtained when solving the first problem showed that  $\eta$  does not change. However, the margin of stable generation of the tractive force



which is characterized by the ratio  $\varepsilon/\varepsilon_{cr}$ , for the sandbox option ( $\varepsilon/\varepsilon_{cr} = 0.081$ ) is 10% better than without it ( $\varepsilon/\varepsilon_{cr} = 0.092$ ).

When solving the problem of a locomotive hitting an oil slick in traction mode, the efficiency of the sand system was analyzed in terms of the response time. In this case, the calculation produced the results similar to those obtained when solving the problem of a locomotive traveling through an oil slick.

The recovery of the traction qualities of the locomotive depends on the sandbox response time. So, in this case, if between the moment of hitting the oil until the moment the sandbox was triggered, the locomotive travels a distance of 60 m, the use of sand makes it possible to stop the slipping process (Fig. 40, a). In the case when the traveled distance is 90 m, the use of sand does not bring the desired results and the slipping would not stop (Fig. 40, b).

Thus, the calculation results confirmed the expediency of the use of a sand system to improve traction.

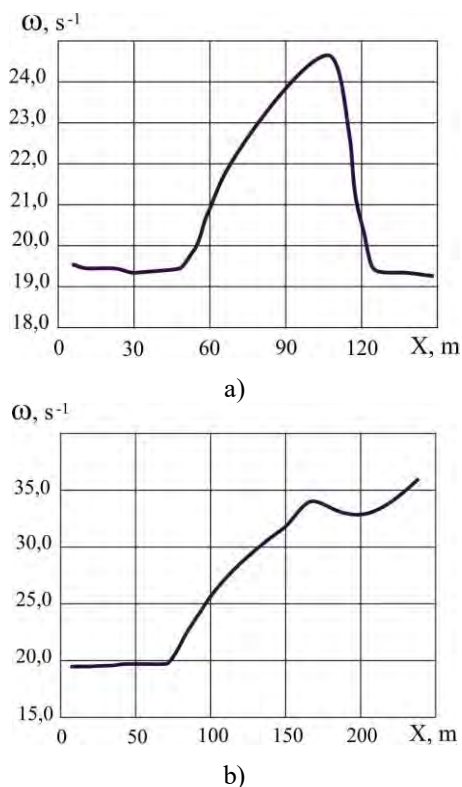


Fig. 40. Travel over an oil slick by a locomotive using a sandbox a) - a slick 60 m long; b) - a slick 90 m long

## **6.5. Analysis of the principles of operation of anti-slipping devices of the locomotive**

Within the framework of the contractual research work carried out by the Department of Locomotive Engineering together with the holding company "Luhanskteplovoz" and dedicated to the development of devices for detecting the difference in rotation speeds of the wheelsets of the traction rolling stock, the author analyzed the basic principles of the anti-slipping devices on locomotives based on the detection of the slipping process by:

- the difference in currents in the electric motor circuits of slipping and non-slipping wheelsets [52, 77, etc.];
- the difference in the rotation speeds of the wheelsets [52, 77, 89, etc.];
- the difference in the slide of the wheelsets [89, etc.];
- the angular acceleration of the wheelsets [52, etc.];
- the absolute slide of the wheelsets [85, etc.].

There are also developments based on the principle of detection of the slipping by frequencies and amplitudes of oscillations in the wheelset drives.

The analysis of the effectiveness of the anti-slipping devices on locomotives that are based on various operating principles was carried out using the suggested locomotive motion model.

Anti-slipping devices must meet some conflicting requirements. On the one hand, they must prevent the excessive slipping of the wheels, while on the other hand, they must enable the locomotive to generate the maximum tractive force determined by the frictional state of the surfaces of the wheels and the rails, which is associated with significant values of slide.

To analyze the performance of anti-slipping devices, the locomotive motion at the maximum power was considered under the following conditions:

- a sharp decline in frictional conditions, i.e. hitting an oil slick was simulated;
- poor adhesion conditions for the first wheelset in the direction of travel, i.e. The first wheelset going into the slipping was simulated;
- persistently poor adhesion conditions, i. e. movement at the limit of adhesion but without going into slipping.

The calculation results showed that when hitting an oil slick, the locomotive enters the runaway slipping mode, i.e. all wheelsets box slipping simultaneously.

The processes of changing the current of traction motors, sliding, the speed of rotation of the wheelsets and the development of auto-frictional vibrations during the slipping occur in the same way for all wheelsets.

Anti-slipping devices based on the principle of comparing the currents in the motor circuits, the speeds of rotation and the slide of the wheelsets do not work. Therefore, to detect the drift skid mode in modern locomotives, additional devices are used that are triggered by the current of the motors, the linear speed of the

wheelset rims of which has reached 105 km/h [77], which at low speeds corresponds to the state of deep slipping (at  $v = 10$  km/h, the value of the relative slide may be as high as hundreds and thousands of percent).

In this case, devices that work according to the principle of individual determination of the degree of slipping of each wheelset of a locomotive are effective, i.e. according to the angular acceleration of the wheelset, while, according to [52], the angular acceleration of  $0.25 \text{ rad/s}^2$  was taken as a criterion for detecting the slipping, according to its absolute slip, according to the level of mechanical vibrations in the drive (occurrence of auto-frictional vibrations).

According to the results of solving the problem a locomotive wheelset going into slipping (locomotive moving at  $v = 10 \text{ m/s}$ ,  $M_t = 14.5 \text{ kNm}$  per wheelset, the high adhesion characteristic at 0.1 for the first wheelset, 0.2 for the remaining wheelsets of a locomotive), anti-slipping devices based on the principle of comparison can detect the slipping process and operate in an efficient manner. In this case, the differences in currents, angular velocities and slide of the wheelsets have significant values (Fig. 41, 42, 43, 44, 45). Devices detecting the slipping by angular acceleration, absolute slide and the level of vibrations in the drive are also effective in this mode (Fig. 43, 44, 45).

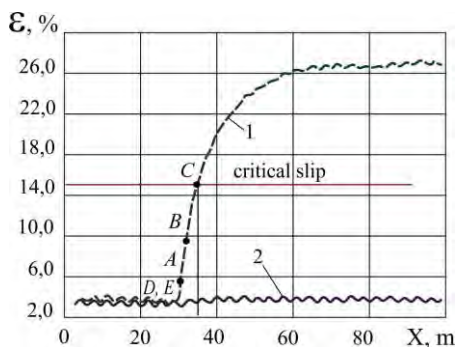


Fig. 41. Change in the relative slide at the slipping of the first wheelset (1 - on the first wheelset, 2 - on the second) when moving in traction mode at maximum power,  $v = 10 \text{ m/s}$  (i.e. A, B, C, D, E - response thresholds for the anti-slipping devices based on the principle of comparing the motor currents, angular velocities of wheel rotation, by the absolute slide, by angular acceleration of the wheel pairs and by the occurrence of auto-frictional vibrations, respectively)

Let us consider the moment of triggering of each device. According to [52], triggering of the anti-slipping device that is based on the principle of comparing the angular velocities of rotation of the wheel pairs will occur when the difference in angular speeds is  $0.5 \text{ s}^{-1}$  (Fig. 41).

Triggering of the anti-slipping device that is based on the principle of comparing the currents in the traction motor circuits occurs when the difference in

currents corresponding at  $v=10$  m/s to the difference in linear velocities at the wheel rims of 0.5 m/s (Fig. 43). According to the experimental studies carried out at the HC "Luhanskteplovoz", the anti-slipping system on the 2TE121 diesel locomotive was triggered when the current difference between the circuits of the motors in the slipping and non-slipping modes reached 100-200 A at the speed of motion 0-15 km/h [30].

Therefore, triggering of the anti-slipping devices that are based on the principle of comparing the currents and angular velocities of rotation of wheelsets will take some time, depending on the settings and sensitivity of these devices.

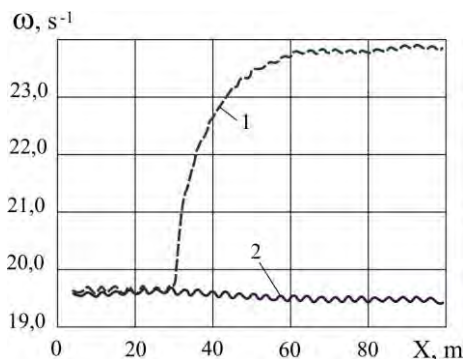


Fig. 42. Change in the angular velocity at the slipping of the first wheelset (1 - on the first wheelset, 2 - on the second) when moving in traction mode at maximum power,  $v=10$  m/s

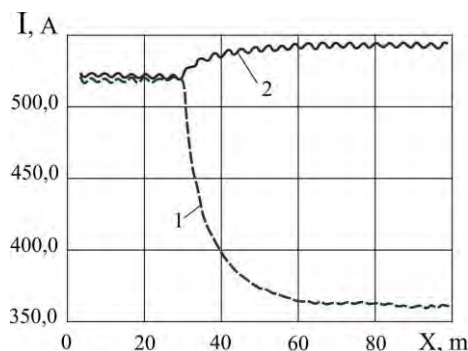


Fig. 43. Change in the motor current at the slipping of the first wheelset (1 - on the first wheelset, 2 - on the second) when moving in traction mode at maximum power,  $v=10$  m/s

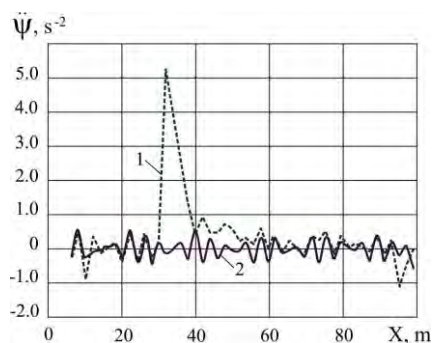


Fig. 44. Change in the angular acceleration of the wheel at the slipping of the first wheelset (1 - on the first wheelset, 2 - on the second) when moving in traction mode at maximum power,  $v=10$  m/s

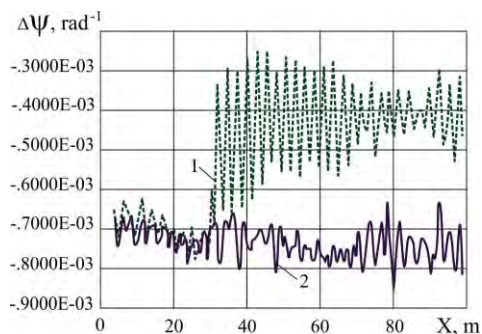


Fig. 45. The development of auto-frictional vibrations of the axles of wheelsets when the first wheelset is slipping (1 - on the first wheelset, 2 - on the second) when moving in traction mode at maximum power,  $v=10$  m/s

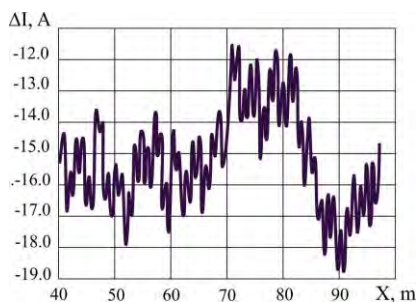


Fig. 46. The difference in currents between the circuits of the 1st and 3rd wheelsets when moving in traction mode at maximum power,  $v=10$  m/s, maximum on the adhesion characteristic 0.15

The development of auto-frictional vibrations in the drive and a sharp increase in the angular acceleration of a wheelset that enters the slipping mode can be recorded simultaneously with the commencement of the slipping process, i.e. almost instantly.

However, the appearance of a higher wheel slip on one or more wheelsets of a locomotive shall not be construed to mean a decrease in tractive force. Experimental studies show that at the moment of generation of the tractive force, the slide of the wheels relative to the rails is 0.8–8% [52, 54, 60, 64, 85], and the spread of these values is contingent on many factors: the magnitude of the tractive force, dynamic processes during the movement, frictional conditions, etc.

Therefore, the triggering of the anti-slipping device that is based on the principle of comparing the currents or speeds of rotation of the wheelsets and adjusted to the above parameters, may occur before the critical slide level is reached, and the power of the locomotive will be underutilized, since the triggering of the anti-slipping device will cause the traction generator to dump the load.

In anti-slipping devices that are based on the detection of the process of auto-frictional vibrations and a sharp increase in the angular acceleration of the wheelset, only the moment of a sharp increase in longitudinal slide is recorded, even though the slide may be far from its critical value, or the longitudinal slide may immediately decrease (if frictional conditions are restored to the same level), and the anti-slipping device is already triggered, and the underutilization of the power of the locomotive in this case is even more likely than in the previous one.

That is why the operation of the anti-slipping device should be based on the traction characteristic, which is adjusted taking into account the real frictional conditions and the speed of movement.

In a device based on the principle of measuring the absolute slide of the locomotive wheels, taking into account the frictional conditions and the speed of movement, it is possible to estimate whether or not the longitudinal slide has reached a critical level, and to fully use the power of the locomotive.

The results of solving the problem of the locomotive motion along the section with consistently poor frictional conditions at maximum power ( $v=10$  m/s,  $M=14.5$  kNm per wheelset, maximum on the adhesion characteristic 0.15) indicate that the difference in current strengths along the motor circuits is 13-16 A (Fig. 49), the obtained values of the difference in the speed of rotation along the wheelsets are 0.2-0.3 rad/s (Fig. 47), the difference in the slide by the wheelsets is 0.5-1.5% (Fig. 49), and auto-frictional vibrations develop in the elements of the wheelset drives.

The results of experimental studies of the wheel slide in electric locomotives operating under conditions of maximum tractive force demonstrate the excessive wheel slide of 4-5% [64], 6-8% [60], 2-4% [54], 0.8-2.5% [52]. For locomotives equipped with a "super-service" anti-slipping system, the adjustments for slide are made within 2-14% [85].

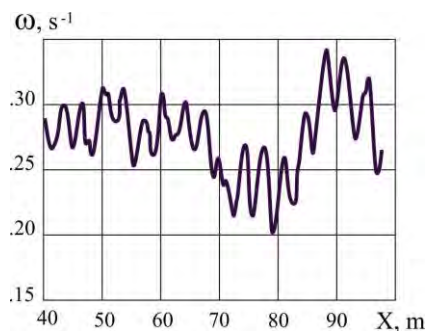


Fig. 47. The difference in angular speeds between the 1st and the 3rd wheelsets when the locomotive moves in traction mode at maximum power,  $v=10$  m/s, maximum on the adhesion characteristic 0.15

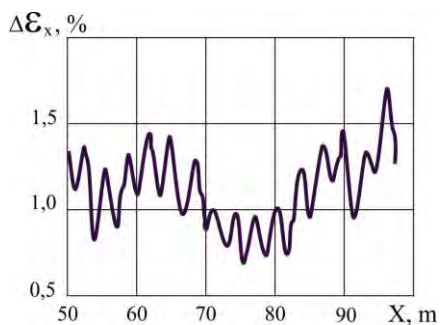


Fig. 48. The difference in longitudinal slide between the 1st and the 3rd wheelsets when moving in traction mode at maximum power,  $v=10$  m/s, maximum on the adhesion characteristic 0.15

Thus, the calculation data are in good agreement with the experimental data.

Based on the results of the performed calculations, the following conclusions were made:

1. The developed mathematical model of the motion of a two-section six-axle locomotive along a straight track section provides a reliable description of the traction and dynamic processes occurring during its travel.
2. The vertical oscillations in the locomotive-railway track system in the simulated coasting motion do not depend on the choice of the adhesion model.

When carrying out the traction-dynamic calculations of the locomotive's motion, especially in traction and braking modes, the adhesion model [18] is recommended to be used, since:

- it most accurately reflects the processes occurring in the contact between the locomotive's wheel and the rail;
- when solving the problem of a locomotive hitting an oil slick in traction mode, i.e. deterioration and then restoration of frictional contact conditions, the use of theoretical models of adhesion [81, 83], which do not have a falling section in their characteristics, leads to incorrect results;
- when using the adhesion models [81, 83], modeling the process of a locomotive starting off with a train of carriages does not reflect correctly the real situation.



## CONCLUSIONS

1. The criteria for assessing the traction and dynamic qualities of locomotives are diverse, and for an unambiguous answer when choosing a design option, several criteria are simultaneously used.
2. For a preliminary assessment of the design of the rolling stock, the use of simple, predominantly static models is justified. A more detailed justification for the decision-making requires more complex, detailed, spatial and dynamic mathematical models.
3. Theoretical studies of a railway vehicle motion shall be carried out on the basis of simulation modeling.
4. Modern trends in the development of traction rolling stock are aimed at both increasing the traction capabilities of locomotives and improving their dynamic qualities.
5. The developed model of the locomotive's motion makes it possible to analyze the efficiency of the slip prevention devices.
6. Anti-slipping devices that are based on the principle of individual determination of the slipping process for each wheelset are more effective than the devices based on the principle of comparing the currents, speeds of rotation and the slide of wheelsets. When setting up anti-slipping devices, in order to fully utilize the power of the locomotive, one shall take into account the effect of frictional conditions on the characteristics of wheel-to-rail adhesion, as well as the difference in the conditions for generation of adhesion forces on each of the wheelsets of the vehicle.

## BIBLIOGRAPHY

1. *Aleksandrov A.I., Grachyov V.F.* Application of the finite element method in the problem of the contact between the wheel and the rail // Problems of dynamics and strength of a railway train: Intercollegiate collection of studies - Dnepropetrovsk, 1981. - Print. 220/28. - p. 116-122.
2. *Asadchenko V.R.* Evaluation of the effectiveness of braking of the vehicles // Bulletin of VNIIZhT. - 1993. - N6. - p. 43-46.
3. *Astakhov P.N.* Resistance to the movement of the railway rolling stock. - M.: Transport, 1966. - 178 p.
4. *Astakhov P.N., Grebenyuk P.T., Skvortsova A.I.* Reference book on traction calculations. - M.: Transport, 1973. - 256 p.
5. *Babikov M.A., Kosinskiy A.V.* Elements and devices of automation. M.: High School, 1975.
6. *Belyaev A.I.* Stochastic stability of the traction drive // Bulletin of VNITL. - 1973. - N 4. - p. 32-35.
7. *Blokhin E.P., Manashkin L.A.* Train dynamics (non-stationary longitudinal vibrations). - M.: Transport, 1982. - 222 p.
8. *Blokhin E.P., Barbas I.G., Manashkin L.A. et al.* Calculation of freight cars for impact strength. - M.: Transport, 1989. - 230 p.
9. *Verigo M.F., Kogan A.Ya.* Interaction of the track and the rolling stock. / eds. M.F. Verigo. - M.: Transport, 1986. - 559 p.
10. *Vershinsky S.V., Danilov V.N., Khusidov V.D.* Car dynamics: A textbook for higher educational institutions of the railway transport / eds. S.V. Vershinsky - 3rd ed., revised and modified. - M.: Transport, 1991. - 360 p.
11. *Vilkevich B.I.* Automatic control of the electric transmission and electric circuits in diesel locomotives. - M.: Transport, 1987. - 272 p.
12. *Garg V.K., Dukkupati R.V.* Rolling stock dynamics. Translated from English / eds. N.A. Pankina. - M.: Transport, 1988. - 391 p.
13. *Golubenko A.L., Tkachenko V.P., Turchin V.P.* Results of the experimental studies of the rubberized wheel prototypes / Voroshilovgrad: VMSI, 1988. - 201 p.
14. *Golubenko A.L.* Wheel-to-rail adhesion. - K.: VIPOL, 1993. - 448 p.
15. *Golubenko A.L.* Enhancing the traction properties of diesel locomotives by improving the mechanical components of the vehicle affecting the adhesion of the wheels to the rails. Thesis of the Doctor of Engineering: 05.22.07 - M., - 1986. - 588 p.
16. *Golubenko A.L., Kramar N.M.* Methods for accounting for forces in the wheel-rail contact zone. // Matters of transport engineering. - Tula: TPI, 1981. - p. 84-90.
17. *Golubenko A.L., Kutsenko S.M., Konyaev A.N.* Fundamentals of the rubberized wheel calculations and the study of their influence on the

- dynamics of the wheel-motor unit // Academic papers of Moscow Institute of Railroad Transport Engineering. - 1973. - Print. 422. - p. 34-50.
18. *Golubenko A.L., Gorbunov N.I., Vivdenko Yu.G.* Influence of tractive force on the dynamic processes during the motion of a rail vehicle / Problems of transport and ways to solve them / Thesis report International scientific and technical conf., - Kyiv, 1994. - p. 107.
  19. *Golubenko A.L., Kostyukevich A.I., Kashura A.L.* Assessment of traction and dynamic qualities of a locomotive at the design stage // Thesis report at the intl. conf. «State and prospects of the development of locomotive building». - Novochoerkassk. -1994. - p. 106-108.
  20. *Golubenko A.L., Kostyukevich A.I., Kashura A.L.* Applicability of various models of adhesion in solving problems of dynamics // Thesis report of the IV intl. scientific and technical conf. «Problems of development of the locomotive building». - Crimea. - 1993. - P.4
  21. *Golubenko A.L., Tkachenko V.P.* Influence of dynamic factors on the process of adhesion and wear in the contact of locomotive wheels with rails / Voroshilovgr. machine building in-t. - Voroshilovgrad., 1983. - 28 p. - Dep. in UkrNIINTI N 393Uk-D84.
  22. *Gorbunov N.I.* Improving the traction qualities of diesel locomotives by improving the elastic coupling of bogies: Abstract of Thesis, Ph.D. Engineering: 05.22.07. - DIIT, Dnepropetrovsk, 1987. - 18 p.
  23. *Danovich V.D., Akhmedov G.G.* Mathematical model of spatial vibrations of the VL85 electric locomotive / Dnepropetr. in-t of r/w transp. engineering. - Dnepropetrovsk, 1990. - Dep. in TsNIITEI MPS N 5456.
  24. *Deev V.V., Ilyin G.A., Afonin G.S.* Traction of trains / eds. V.V. Deev V.V. - M.: Transport, 1987. - 234 p.
  25. *Demin Yu.V., Kovtun E.N.* Study of the forced lateral vibrations of rail vehicles with dry friction dampers. Academy of Sciences of the Ukrainian SSR, Institute of technical mechanics, Dnepropetrovsk, 1983. - 25 p. Dep. No. 3893-83.
  26. *Demin Yu.V., Dlugach L.A., Korotenko M.L., Markova O.M.* Self-oscillations and motion stability of rail vehicles. - K.: Nauk. dumka, 1984. - 160 p.
  27. *Demchenko I.P.* Computer study of longitudinal vibrations of a biaxial bogie / Electric locomotive building. - Novochoerkassk, 1993. - vol. 33. - p. 109-117.
  28. *Demchenko I.P.* Impact of longitudinal couplings of the bogies with the box on the dynamic properties and generation of the tractive force in electric locomotives. Thesis ... Ph.D. In Engineering. - M., 1993. - 163 p.

29. *Demchenko I.P., Sergienko P.E.* Longitudinal dynamics of a carriage with inclined rods // Thesis report IV intl. scientific and technical conference "Problems of development of locomotive building". - Crimea, 1993.
30. Dynamic and strength tests of the traction drive of wheelsets of the diesel locomotive 2TE121-002B on the tracks of the Ministry of Railways: Research report (final) / PKTI; OIP N 20-81; Voroshilovgrad, 1981. - 149 p.
31. *Evstratov A.S.* Locomotive running gear. - M.: Mechanical engineering, 1987. - 136 p.
32. *Evstratov A.S.* Dynamic loads of the locomotive running gear from vibrations of unsprung parts and their reduction: Thesis ... Doctor of Engineering: Kolomna, 1983. - 371 p.
33. *Yelbaev E.P.* On the problem of the nature of the movement of the wheelset in the curved sections of the railway track / Kharkov Polytechnic. in-t. - Kharkov, 1989. - 25 p. Dep. in VNITI No. 499.
34. *Zevenhoven N.* Experimental study of the adhesion of a driving axle with a three-phase current drive. // Railway transport. - 1981. - N12. - p. 7-18.
35. *Isaev I.P., Golovaty A.T.* Traction calculation rules need revision // Locomotives. -1992. - N8. - p.
36. Investigation of lateral vibrations of a single-carriage model of a subway car on a digital computing machine: R&D Report / MIIZhT; - No. 26-U80. - Moscow, 1980. - 77 p.
37. Investigation of the influence of operating conditions and the state of the undercarriage on the wear of the ridges of non-pedestal bogies of freight diesel locomotives; Research report / VNITI; No. I-4786. - Kolomna, 1986. - 89 p.
38. *Kalker I.I., Pater A.D. et al.* Review of the theory of the local slide in the area of elastic contact with dry friction // Applied Mechanics. - M., 1971. - vol. 7. - Issue 5. - p. 9-20.
39. *Kovalyov N.A.* Free movement of a two-axle carriage with Coulomb friction between the wheel and the rail. Vestnik VNIIZhT. - 1957. - No. 4. - p. 93-97.
40. Construction, calculation and design of locomotives / eds. Kamayev V.A. - M.: Mechanical engineering, 1981. - 351 p.
41. *Kostyukevich A.I.* Numerical and experimental identification of the process of adhesion of locomotive wheels to rails: Thesis ... Ph.D. In Engineering: - Luhansk, 1991. - 232 p.
42. *Kravchenko A.I., Sergienko P.E., Yanov V.P.* On the traction drive of a promising locomotive // Railway transport. - 1982. - No. 4. - p. 53-55.
43. *Kramar N.M.* Lateral horizontal vibrations of a locomotive on rubberized wheelsets: Thesis ... Ph.D. In Engineering: 05.22.07. - Voroshilovgrad, 1983 - 215 p.

44. *Krettek O.* Modern achievements in the study of the problem of adhesion // World Railways. - 1974. - No. 10. - p. 3-16.
45. *Kuzmich V.D.* On the traction parameters of freight diesel locomotives / Railway transport. Ser. Locomotives. State and prospects for the development of locomotive traction. M.: TsNIITEI MPS, 1992. - Print. 2. - P.1-9.
46. *Luvishis A.L.* Trends in the development of the US diesel locomotive fleet // Railway transport. - 1997. - No. 3. - p. 73-77.
47. *Lvov N.V.* Impact of some parameters of the mechanical part of the EPS on generation of the tractive force: Thesis ... Ph.D. In Engineering: - M., 1979. - 154 p.
48. *Manashkin L.A., Granovsky R.B.* On the modeling of periodically repeating disturbances in the movement of a rail vehicle. - M.: Science, 1975. - 60 p.
49. *Markovichenko V.V.* A mathematical model of horizontal dynamics of a railway carriage moving along a straight path, taking into account the tractive force // Coll. Improving the dynamic qualities of rolling stock and trains in the Siberian region. - Omsk, 1989. - p. 44-51.
50. *Ushkalov V.F., Reznikov L.M., Ikkol V.S., Trubitskaya E.Yu., Redko S.F., Zaleskiy A.I* Mathematical modeling of oscillations of rail vehicles / eds. V.F. Ushkalov - Kyiv: Naukova Dumka, 1982, 240 p.
51. *Biryukov I.V., Savoskin A.N., Burchak G.P. et al* Mechanical part of the traction rolling stock: A textbook for higher educational institutions of the railway transport / eds. I.V. Biryukov. - M.: Transport, 1992. - 440 p.
52. *Minov D.K.* Improving the traction properties of the electric and diesel locomotives with electric transmission. M.: Transport, 1965. - 267 p.
53. *Neymark Yu.I., Fufayev N.A.* Dynamics of non-holonomic systems. M.: Science, 1967. - 519 p.
54. *Nekrasov A.O., Muginstein L.A., Khatskelevich A.A., Andreyev A.V.* Patterns of dynamic distribution of the loads between traction motors / VNIIZhT Bulletin. - 1992. - No. 2. - p. 38-42.
55. *Pavlenko A.P.* Impact of the type and parameters of the traction drive on the stability the locomotive motion along the straight sections of the track // Thesis report conf. «Problems of mechanics of railway transport: Enhancing the reliability and improving the design of the rolling stock». - Dnepropetrovsk. - 1984. - p. 86.
56. *Pavlenko A.P.* Influence of dynamic processes in the traction drive on the stability of the locomotive motion // Trudy RIIZhTa. - Rostov-on-Don, 1984. - Print 1976. - p. 3-10.
57. *Pavlenko A.P.* Dynamics of the traction drives of mainline locomotives. - M.: Mechanical engineering, 1991. - 192 p.

58. Locomotive Sandbox: Inventor's Certificate No. 1781112./ *Gorbunov N.I., Kashura A.L., Mikhaylov E.V., Golubenko A.L., Kudla P.I., Mogila V.I., Osenin Yu.I.* Printed on 12/15/92. Bul. 46. - 3 p.
59. Locomotive Sandbox: Inventor's Certificate 1770188 USSR, MKI V61 S 15/10 / *N.I. Gorbunov, E.V. Mikhaylov, A.L. Kashura, P.I. Kudla, A.S. Klyuev, V.I. Mogila.* No. 4890808/11; Stated 10.17.90; Publ. 10/17/92, Bul. No. 39. - 3 p.
60. *Pokrovsky S.V.* Impact of the rigidity of traction characteristics on the efficiency of using the potential coupling of electric locomotives / Bulletin of VNIIZHT. - 1992. - No. 1. - p. 42-46.
61. *Popp K.* Simulation of the track structure. // Dynamics of high-speed transport: Translated from English by A.V. Popov / Ed. T.A. Tibilov. - M.: Transport. 1988. - p. 15-31.
62. Traction calculation rules for train operation: Approved by the Ministry of Railways of the USSR 15.08.80. - M.: Transport, 1985. - 287 p.
63. Development of locomotive traction / Ed. N.A. Fufryanskiy and A.N. Bevzenko. - M.: Transport, 1982. - 303 p.
64. Operating modes of mainline electric locomotives / *O.A. Nekrasov, A.L. Lisitsyn, L.A. Muginstein, V.I. Rakhmaninov* / eds. O.A. Nekrasov. M.: Transport, 1983. - 231 p.
65. *Rosenfeld V.E., Isaev V.P., Sidorov N.N.* Electric traction theory. - M.: Transport, 1983 - 328 p.
66. *Savoskin A.N., Burchak G.P., Dorgachev N.I.* Investigation of the influence of a traction drive on vertical vibrations of an electric locomotive // Problems of dynamics and strength of the railway rolling stock. - Dnepropetrovsk, 1982. - p. 53-58.
67. Comparative dynamic tests of locomotives 2TE116A-001 and 2TE116-517; R&D / PKTI Report; OIP 2-82. - Voroshilovgrad, 1982. - 65 p.
68. *Tkachenko V.P.* Traction qualities of a locomotive with rubberized wheelsets: Thesis ... Ph.D. in Engineering: 05.22.07 Voroshilovgrad, 1983. - 216 p.
69. Brake linkage of a three-axle locomotive bogie: Inventor's Certificate 1675144 USSR, MKI V61 N 13/10 / *N.I. Gorbunov, E.V. Mikhaylov, A.L. Kashura, A.L. Golubenko, A.M. Morozov, V.I. Mogila, P.Yu. Kramarenko.* No. 4707697/11; Stated 06/19/89; Publ. 9/7/1991, Bul. No. 33. - 4 p.
70. Brake linkage of a three-axle locomotive bogie: Inventor's Certificate No. 1799769. / *Gorbunov N.I., Mikhaylov E.V., Mogila V.I., Kashura A.L.* Publ. 07.03.93 Bul. 9. - 3 p.
71. A device for controlling the traction motors of a vehicle. *Gorbunov N.I., Mikhaylov E.V., Kashura A.L., Tasang E.Kh., Grinevich V.P., Novikov V.M.* / Positive decision on application N 4795838/11.

72. *Ushkalov V.F., Malysheva N.Yu.* Influence of the choice of the creep model on the joint spatial oscillations of the rail vehicle and the elastic-dissipative inertial track // Oscillations and dynamic qualities of railway rolling stock. - Dnepropetrovsk, 1989. p.10-21.
73. *Ushkalov V.F., Malysheva N.Yu.* Calculation of creep parameters in solving the problems of interaction between the wheel and the rail. Oscillations of complex mechanical systems. - K., 1990. - p. 48-58.
74. Locomotive sandbox nozzle: Inventor's Certificate 1801827 USSR, MKI V61 S 15/10. / *N.I.Gorbunov, E.V. Mikhaylov, A.L.Kashura, P.I.Kudla, A.L. Golubenko, V.I.Mogila.* No. 4879350/11; Stated 09.17.90; Publ. 3/15/1993, Bul. No. 10. - 3 p.
75. *Khusidov V.D., Petrov G.I., Strogova O.I. et al.* Mathematical and software support for calculating the dynamic properties of freight cars with various schemes of running gears. M., 1990. - 62 p. - Dep. in TSNIITEI TYAZHMASH, N 5377.
76. *Chernyak A.Yu.* Forecasting the dynamic loading of six-axle diesel locomotives and determining the rational parameters of the horizontal coupling of the running gears: Thesis ... Ph.D. In Engineering: Dnepropetrovsk, 1988. - 252 p.
77. Electric equipment of diesel locomotives. Reference book / *V.E. Verhoglyad, B.I. Vilkevich, V.S. Marchenko et al.* / eds. V.S. Marchenko. - M.: Transport, 1981. - 287 p.
78. *Rotanov N.A., Kurbasov A.S., Bykov Yu.G., Bykov V.V.* Litovchenko / eds. N.A. Rotanov. - M.: Transport, 1991. - 336 p.
79. *Yakushev V.V.* Study of the forces of interaction between the wheel and the rail and taking them into account in the problems of lateral vibrations of the car: Thesis ... Ph.D. In Engineering: Bryansk, 1976. - 214 p.
80. *Yakushev V.V.* On the problem of the relationship between the longitudinal and transverse forces of the creep // Problems of the mechanics of railway transport. - Dnepropetrovsk, 1984. - p. 93.
81. *Chartet A.* La Theorie Statique de Derailment d'un Essieu-Revue generale les chemins de fer, 1950, v. 69, pp. 57-63.
82. *Frederich F.* Beitrag zur Untersuchung der Kraftschubbeanspruchungen an schragrollenden Schienenfahrzeugradern. Dr.-Ing. dissertation, Berlin, 1969. - 89s.
83. *Kalker J.J.* Survey of Wheel-Rail Rolling Contact Theory. - Vehicle System Dynamics, 1979, v8, N 4, p.317-379.
84. *Koffman I.L.* Gummigefederte Lokomotivrader. - DET, 1974, 22, Nr1, s.27-30.

85. *Meyer B.R.* High-adhesion locomotives with controlled creep. "Proc. Inst. Mech. Eng.: Int. Conf. Diesel Locomot. Future, York, 7-9 Apr. 1987 ". London, 1987, 209-218.
86. *Muller T.* Kraftwirkungen an Zweiachsigen Triebgestall bei Antrieb der Radsatze durch Ge Gelenkwellen // Glasers Ann. - 1961. - 85, N 6. - S. 203-209.
87. *Oraszvary L., Szilagyi G.* Szabadon gordulo vasuti kerekpar mozgasanak Virsgalata // Evsk. 1990 / Vasuti Tud. kut. intez.
88. *Pocklington A.R.* Effects of lateral forces when propelling round shlap curves. - Railway Gas, 1965, 121, Nr 23, p.942-945.
89. Układ napędowy zapewniający samoczynną lokwidację poslizgu zestawów kołowych: [Ref.] 5 Konf. nauk. SEMTRAK'92 / Gizinski Z. // Monogr. / PKrak. - 1992. - N137. - C.107-114.
90. Zwischen Rad und Schiene / Dautzenberg J. // Deine Bahn. - 1992. - 20, N2. - S. 95-97.



**Initial data for the diesel locomotive 2TE116 calculations**

Name	Size	Unit of Measurement
1	2	3
1. Half the distance between the wheel rolling circles	0.79	m
2. Half the distance between the axle boxes in the transverse direction	1.067	m
3. Distance between the axle boxes in the bogie in longitudinal direction	1.85	m
4. Half the distance between the supports in the transverse direction	1.067	m
5. Half the distance between the supports in the bogie in the longitudinal direction	0.9	m
6. Half the distance between the supports in the locomotive in the longitudinal direction: external internal	5.9 4.1	m m
9. Axle box clearances in the bogie: for a new locomotive taking into account wear and tear	2-14-2 5-14-5	mm mm
7. Distance between the axle and the traction electric motor suspension	0.924	m
8. Distance between the axis and the center of gravity of the traction electric motor	0.462	m
9. Distance between the center of the bogie and the center pin	0.185	m
10. Distance between the center of the body and the center pin	4,815	m
11. Height from the center pin to the automatic coupler	0.055	m
12. Wheel radius in a rolling circle	0.525	m
13. Axial gear ratio	4.42	m
14. Wheelset mass	1805	kg
15. Traction motor mass	3250	kg
16. Bogie mass	6350	kg
17. Body mass	88,000	kg
18. Moments of inertia about the OX axis: wheelset motor bogie body	2,000 480 3,570 185,000	kgm <sup>2</sup> kgm <sup>2</sup> kgm <sup>2</sup> kgm <sup>2</sup>
19. Moments of inertia about the OU axis: wheelset motor	900 286	kgm <sup>2</sup> kgm <sup>2</sup>

armature	26.3	kgm <sup>2</sup>
bogie	8,050	kgm <sup>2</sup>
body	140,000	kgm <sup>2</sup>

C o n t i n u e d

1	2	3
20. Moments of inertia about the OZ axis:		
wheelset	2,000	kgm <sup>2</sup>
motor	980	kgm <sup>2</sup>
bogie	300	kgm <sup>2</sup>
body	148,000	kgm <sup>2</sup>
21. Reduced mass of the rail	400	kg
22. Stiffness of the axle suspension elements (per one axle):		
longitudinal	53,000	kN/m
transverse before taking up the elastic play	0	kN/m
transverse after taking up the elastic play	8,000	kN/m
vertical	754	kN/m
23. Stiffness of the elements of the second stage of spring suspension (per one support):		
transverse	200	kN/m
vertical	5,520	kN/m
24. Traction electric motor suspension stiffness:		
transverse	12	kN/m
vertical	4,000	kN/m
25. Pivot stiffness:		
with a clearance of up to 20 mm	0	kN/m
with a clearance of more than 20 mm up to 40 mm	400	kN/m
26. The restoring moment of the second stage of the spring suspension	22.4	kN/rad
27. The angle before the selection of the clearance in the return apparatus	0.0524	rad
28. Rail stiffness:		
vertical	49,000	kN/m
transverse	10,000	kN/m
29. Coefficients of viscous resistance of axle suspension elements (per one axle):		
longitudinal		
transverse before taking up the elastic play	9.25	kNs/m
transverse after taking up the elastic play	0	kNs/m
vertical	46	kNs/m
	20.5	kNs/m
30. Coefficients of viscous resistance of elements of the second stage of spring		

suspension (per one support):		
transverse	0.1	kNs/m
vertical	185	kNs/m

C o n t i n u e d

1	2	3
31. Traction motor suspension viscous resistance coefficients:		
transverse	0.1	kNs/m
vertical	1	kNs/m
32. Coefficients of viscous resistance of the pivot apparatus:		
with a clearance of up to 20 mm	0	kNs/m
with a clearance of more than 20 mm up to 40 mm	0	kNs/m
33. Coefficients of viscous resistance of the rail thread		
vertical	220	kNs/m
transverse	80	kNs/m

# SCIENTIFIC PUBLICATION

Monograph

## DEVELOPMENT AND EVALUATION OF TECHNICAL SOLUTIONS TO INCREASE THE QUALITATIVE LEVEL OF THE LOCOMOTIVE UNDERCARRIAGE

Authors:

Mykola Ivanovych GORBUNOV,  
Maksym Volodymyrovych KOVTANETS,  
Oksana Viktorivna SERHIENKO,  
Tatiana Mykolaevna KOVTANETS

Authorized for printing 06.12.2021.

Print format 60x84 1/16. Printing paper. Times Font.

Offset printing. Printer's sheet 5.7. Publisher's sheet 7.2.

Run of 50 copies. Issue No. 5426. Order No. 18. Contracted price.

The V. Dahl East Ukrainian National University Press

Address of the publishing house: 93400, Severodonetsk, Luhansk region.

59a Central avenue, main building

telephone: +38 (050) 218 04 78, fax (06452) 4 03 42

E-mail: vidavnictvosnu.ua@gmail.com

